U-Pb zircon ages, mapping, and biostratigraphy of the Payette Formation and Idaho Group north of the western Snake River Plain: implications for hydrocarbon system correlation

R.L. Love[1], R.S. Lewis[2], S.H. Wood[3], D.M. Feeney[2] and M. D. Schmitz[4]

[1] Department of Geosciences, University of Idaho, 875 Perimeter Drive MS 3022, Moscow ID 83844-3022; rlove@uidaho.edu

[2] Idaho Geological Survey, University of Idaho, 875 Perimeter Drive MS 3014, Moscow, ID 83844-3014; reedl@uidaho.edu, dmfeeney@uidaho.edu

[3] Boise State University, Environmental Research Bldg. 1160 MS 1535, Boise ID 83725; swood@boisestate.edu

[4] Department of Geosciences, Boise State University, 1910 University Drive, Boise ID 83725; markschmitz@boisestate.edu

This paper is a non-peer reviewed preprint submitted to EarthArXiv. The article is currently under review with the Journal of Sedimentary Research.

ACKNOWLEDGEMENTS

The authors would like to thank Mark Barton for discussions regarding the sequence stratigraphy of the oil and gas fields of southwest Idaho, Patrick Fields and William Rember for helpful discussions about plant micro- and macrofossils, and Nate Carpenter for discussions on Lake Idaho. Finally, we would like to thank the numerous landowners in the Emmett and Payette area for access, without which, this report would not have been possible.

ABSTRACT

The sedimentary deposits north of the western Snake River Plain host Idaho's first and only producing oil and gas field. They consist of the mid-Miocene Payette Formation, the mid-late Miocene Chalk Hills Formation, and the Pliocene to early Pleistocene Glenns Ferry Formation. Using new geochronology, palynomorph biostratigraphy, and geologic mapping, we connect up-dip surface features to subsurface petroleum play elements. The Payette Formation is potentially the source of the hydrocarbons and acts as one of the reservoirs in the basin. Here we redefine the Payette Formation as 900 m of mudstone with lesser amounts of sandstone overlying and interbedded with the Columbia River Basalt Group and Weiser volcanics. Index palynomorphs, including *Liquidambar* and *Pterocarya*, present in Idaho during and immediately after the mid-Miocene climatic optimum, and new U/Pb dates of 16.39 and 15.88 Ma, help establish the thickness and extent of the formation. For the first time, these biostratigraphic markers have been defined for the oil and gas wells. The Chalk Hills Formation is a tuffaceous siltstone, claystone, and sandstone that is ~300 to 520 m thick. U/Pb dates are 9.00, 9.04, and 7.78 Ma. The Chalk Hills Formation acts both as a reservoir and the sealing mudstone facies. The overlying siltstone to fine conglomerate of the Glenns Ferry Formation acts as the overburden and sealing facies to the petroleum system in the subsurface but was important to the formations burial and hydrocarbon maturation. Both the Chalk Hills and Glenns Ferry Formation were deposited within ancient Lake Idaho during an overall increase in aridity and cooling after the mid-Miocene climatic optimum.

INTRODUCTION

Miocene and younger sedimentary deposits are exposed within and on the flanks of the western Snake River Plain (WSRP; Figs. 1 and 2). Fluvial and lacustrine depositional systems existed here in southwest Idaho and adjacent southeast Oregon from the middle Miocene to early Pleistocene. The resulting sediments have been named the Miocene Payette Formation (Lindgren, 1898; Kirkham, 1930) and the Idaho Group comprised of the late Miocene Poison Creek and Chalk Hills Formation and the Pliocene Glenns Ferry Formation (Malde and Powers, 1962; Wood and Clemens, 2002). Previous research has focused on the area south of the plain, particularly the well-exposed sections of the Chalk Hills Formation and Glenns Ferry formations near Bruneau, Idaho (Kimmel, 1979, 1982; Swyridczuk, 1979, 1980a, 1980b; Smith et al., 1982).

Kirkham (1930) used the name Payette Formation to refer to beds, mostly on the north side of the WSRP, which are interbedded with Miocene volcanic rocks. These include basaltic to andesitic rocks of the lower Columbia River Basalt Group (CRBG) and basaltic to rhyolitic rocks of the Weiser volcanics (Fitzgerald, 1982; Reidel et al., 2013). In this paper we expand that definition to include a sequence of beds immediately overlying the CRBG and Weiser volcanics (Fig. 2). The Payette Formation has regional paleoclimate significance because our study indicates deposition was contemporaneous with part of the global mid-Miocene climatic optimum (Zachos et al., 2001; Kosbohm and Shoene, 2018).

The depositional extent of the Payette Formation sediments appears to differ from the Late Miocene Idaho Group but is not yet well defined. The Sucker Creek Formation on the south side of the plain has similarities and is of the same age (Forester and Wood, 2012; Nash and Perkins, 2012). After a depositional hiatus, accommodation for the Idaho Group sediments is associated with the rifting and subsidence of the WSRP and the resulting paleolake systems. The Glenns Ferry and Chalk Hills formations are associated with the most extensive and recent lake called Lake Idaho. The demise of this lake occurred when it overflowed (~2.7 to 2 Ma) at a low point near Huntington, Oregon and was captured by the Salmon-Columbia River system resulting in the downcutting of Hells Canyon of the Snake River (Wheeler and Cooke, 1954; Hearst, 1999; Wood and Clemens, 2002).

Our mapping, geochronology, palynology, and subsurface study of recent petroleum wells provides new information on the stratigraphic section that includes volcanic and sedimentary rocks on the north side of the WSRP in Payette, Gem, and Washington counties. This area has previously been termed the West Idaho basin, Payette basin, and Weiser basin (Bond et al., 2011; Breedlovestrout et al., 2017; Breedlovestrout and Lewis, 2017). Although the Payette Formation is overlain by the Idaho Group stratigraphically, the basins developed from two separate, and most likely different, phases of accommodation. The Payette Formation deposition may be linked to the north-south trending normal faults that are persistent throughout western Idaho and eastern Oregon (including the Sucker Creek Formation and Ore-Ida graben; Cummings et al., 2000). The Idaho Group deposition is associated with a series of northwest-southeast faults that down-drop toward the western Snake River Plain. Here we collectively call the package of Payette and Idaho Group sediments as deposited in “the basin” but recognize that there are two different phases of basin development that may be related to different structural mechanisms. The basin has received recent attention because it is the focus of hydrocarbon production that began with the successful wildcat well, ML Investment 1-10, drilled by Bridge Resources in

2010 near New Plymouth, Idaho (Fig. 3). In 2015, Idaho became a petroleum producing state for the first time when 6 wells in Payette County started producing gaseous and liquid hydrocarbons from thle Payette Formation. By the end of 2018, 23 total wells had been drilled and 16 of them produced hydrocarbons. The field is now operated by High Mesa Holdings and Snake River Oil and Gas.

In this study, we present a summary of results from geologic mapping initiated in 2013 by the Idaho Geological Survey as part of the U.S. Geological Survey National Cooperative Geologic Mapping Program. This mapping was a response to the successful hydrocarbon exploration efforts and was designed to give an up-dip perspective on the new fields. In addition, a better understanding of the stratigraphy was considered valuable for potential hydrogeologic studies related to hydrocarbon extraction. Mapping was augmented by paleobotany and zircon U-Pb age determinations. A primary goal of this work is the reconciliation of prior stratigraphic interpretations with our mapping, paleobotany, and geochronology. Mapping and basin characterization studies are ongoing, including whole-rock X-ray fluorescence analyses (XRF) of volcanic rocks (eg Feeney and Schmidt, 2019) and sequence stratigraphy (Barton, 2019).

GEOLOGIC SETTING AND DEPOSITIONAL CONDITIONS

Pre-Miocene rocks

Rocks in the subsurface of the basin are known only from well data and from mapping on the eastern flank of the area (Fig. 3 and 4). A geothermal well on the northernmost extent of the basin, Chrestesen No. A-1, drilled approximately 9 mi (15 km) east-northeast of Weiser encountered likely Mesozoic accreted island arc lithologies 1829 m deep in the subsurface (greenstones, possibly from the Seven Devils Volcanic Group; Bond et al., 2011). The eastern boundary of the accreted terranes is not exposed but likely lies east of the basin, east of Emmett, Idaho (Fig. 1). The edge of the accreted terranes is marked by a change in initial $^{87}Sr/^{86}Sr$ which increases from values of 0.704 or less in the west to values of 0.706 or more in the east (Armstrong et al., 1977; Benford et al., 2010). Steep foliation developed along the terrane boundary may have influenced later north-south faults that controlled the initial deposition of the Payette Formation. East of the accreted terrane rocks are granitic rocks of the Late Cretaceous Idaho batholith.

Miocene and younger volcanism

The middle Miocene in northern Nevada, southeast Oregon, and southwest Idaho was host to the coeval emergence of the Yellowstone hotspot and the flood basalts of the CRBG (Morgan, 1972; Swanson et al., 1979; Reidel et al., 1989; Smith and Braile, 1994; Camp and Ross, 2004; Benson et al., 2017). Silicic volcanism of the Yellowstone hotspot began at 16.5 Ma at the McDermitt caldera complex in northern Nevada (Mahood and Benson, 2017). As the North American plate migrated southwest, the Yellowstone hotspot left behind a succession of silicic tuffs and flows, topographic highs, and complex caldera systems (Pierce and Morgan, 1972; Bonnichsen and Kauffman, 1987). The CRBG initiated at 17.23 Ma with the Picture Gorge basalts erupting along the Monument dike swarm in eastern Oregon (Cahoon, et al., 2020), followed at 16.6 Ma by the Steens Basalt in southeast Oregon (Camp et al., 2013), leading to the main phase of volcanism, Imnaha Basalt, Grande Ronde Basalt, Wanapum Basalt erupting from the Chief Joseph dike swarm in northeastern Oregon, southeastern Washington and western Idaho (Hooper et al., 2007, Barry et al., 2013). Recent dates from Kasbohm and Schoene (2018) suggest 95 percent of the CRBG volume erupted from 16.7 Ma to 15.9 Ma.

Volcanism north of the WSRP (Figs. 1 and 3) includes marginal flows of the Steens, Imnaha, and Grande Ronde basalts of the CRBG, iron-rich andesite flows conformable to CRBG that are typically associated with rhyolite blocks and dikes, and silicic ash fallout from regional volcanism (Fitzgerald, 1982; Feeney et al., 2016b, 2017). The CRBG and the iron-rich andesite are unconformably overlain by the Weiser volcanics, a small field of calc-alkaline to slightly tholeiitic effusive flows ranging from rhyolite to basalt (Fitzgerald, 1982; Feeney et al., 2016b) that erupted from 15.4 Ma to 14.9 Ma (R. Gaschnig, 2015 and M. Schmitz, 2018, personal communication). The thickest exposure of Weiser volcanics is 500 m northeast of Weiser River (Feeney et al. 2016b); the base is not exposed, however, and this thickness includes Payette Formation sedimentary interbeds. Likewise, the underlying CRBG flows are also interbedded with the Payette Formation. The Weiser volcanics thin southward to the Paddock Valley Reservoir and are absent south of it (Fig 3). Additional thin and isolated volcanic flows and sills are identified in wells near the Oregon-Idaho border (Wood, 2019); these volcanics are neither temporally or geochemically correlative to CRBG or Weiser volcanics. The youngest volcanism in the region is the latest Tertiary to Quaternary WSRP style of volcanism (QTb on Fig. 1) which includes lava flows, cinder cones, shield volcanos, and maar-like vents erupting on to wet sediments and Snake River plain fluvial gravels (Shervais et al, 2002; Bonnichsen et al., 2016; Rivera et al., 2021).

Structure

The oldest structures in the study area are north-south trending normal faults related to the larger western Idaho fault system (Figs 1 and 3; Capps, 1941; Fitzgerald, 1982; Knudson et al., 1996), which are interpreted to have provided initial basin accommodation for the Payette Formation. These faults resulted in large fault-bound rotational blocks of repeated basalt flows. These faults are 5 to 55 km (3 to 35 mi) long and offsets are up to 1000 m (Fitzgerald, 1982). Offset ash in Quaternary fan deposits indicate continued fault activity into the late Holocene (Gilbert et al., 1983). The second type of faulting in the area are northwest-trending normal faults of the Paddock Valley fault zone (Fig. 3). No evidence of Quaternary movement has been found along these structures. The zone is up to 10 km (6 mi) long and offsets of hundreds of meters occurred from middle to late Miocene (Fitzgerald, 1982). Fitzgerald (1982) postulates that the Paddock Valley fault zone accommodated the fissures of the Weiser volcanics. Lastly, two east-west normal faults of uncertain age are present northeast of Weiser (Feeney and Schmidt, 2019) and speculative structures along Big and Little Willow creeks are of similar orientation (Fig. 3). Subsidence of the basin has resulted in the current geometry whereby the strata have an overall southwest dip (Figs. 3 and 4).

Early Sedimentation: Payette Formation

The CRBG and rhyolitic volcanism created a new landscape that changed the drainage patterns and resulted in a series of small lakes and fluvial watersheds throughout the Inland Northwest.

The sedimentary deposits formed in this landscape are now represented by the age correlative Latah Formation of the eastern Washington and northern Idaho (Pardee et al., 1925; Kirkham and Johnson, 1929; Smiley, 1989; Smiley and Rember, 1985), the Sucker Creek Formation of southeast Oregon and southwest Idaho (Taggart et al., 1980; Fields, 1996), the Payette Formation of southwestern Idaho (Lindgren, 1898; Bowen, 1913; Buwalda, 1924; Kirkham, 1931) and the Mascall Formation of central Oregon (Bestland et al., 2008). These units were deposited during and after the mid-Miocene climatic optimum, which lasted from ~17-15 Ma (Zachos et al.; McKay et al., 2014). The Payette Formation is the oldest sedimentary in the basin (Figs. 2, 3, and 4) and is likely a contributor as a hydrocarbon source and reservoir for the oil and gas play (Warner, 1975; Bond et al., 2011).

Paleoclimate of southern Idaho was much warmer during the Miocene compared to today and a temperate, broadleaved forest ecosystem was dominant (Leopold and Denton, 1987; Mustoe and Leopold, 2014). Numerous plant fossil localities in the Payette Formation are associated with this climatic optimum.

The Payette Formation was originally defined as the oldest part of the sedimentary sequence by Lindgren (1898), who noted that it was typically deformed and overlain by the less-deformed Idaho Formation (now Idaho Group). His comment in a footnote (p. 632) “to separate the deposits of the two formations is not always easy” is one we heartily agree with, but an approximate contact is now recognized by our mapping and dating efforts northwest of Emmett (Fig. 3). The relationship of the Payette Formation to the CRBG has been uncertain. Several authors, including Lindgren (1898) have suggested that the Payette is interbedded with and overlies the CRBG. In contrast, Kirkham (1931) suggested that the Payette Formation should only include the interbeds within and that underlie the CRBG while the sedimentary package above the CRBG should be regarded as the Poison Creek Formation. Sediments were estimated to have a maximum age of approximately 17 Ma based on fossil flora biostratigraphy (Smiley et al., 1975b). The age of the lower part of the Payette Formation can be constrained by the more precise absolute age of the dated volcanic units it is interbedded with, including CRBG flows erupted between 16.9 and 15.9 Ma and 15.4 to 14.9 Ma Weiser volcanic flows (Kasbohm and Schoene, 2018 Jarboe et al., 2010; Feeney et al., 2017). The minimum age is not well constrained but is approximately in the range of 14 to 12 Ma (Breedlovestrout and Lewis, 2017; Breedlovestrout et al., 2017; Barton, 2019).

Lindgren (1898) estimated the thickness of the Payette Formation to be ~300 to 366 m in the type sections north of Boise near Horseshoe Bend (HSB in Fig. 1). There the Payette Formation consists of interbedded sandstone, claystone, siltstone, carbonaceous shale, coal, and local conglomerate (Fig. 6). The coal occurs as thin beds 2.5 cm to ~1 m and is subbituminous and lignitic in maturity (Bowen, 1913). Numerous plant fossil localities are present in the Payette Formation. Fields (1983) examined macroflora in some of the organic-rich layers from the type section of the Payette Formation near Horseshoe Bend and documented dominantly *Populus, Quercus*, *Salix*, and *Taxodium*. Other less common paleoflora are *Pinus, Picea, Abies, Pseudotsuga, Acer*, *Fagus*, and *Thuja*. Shah (1966, 1968) also studied macrofossils near Weiser and identified these common paleofloras. These floras document a temperate, broadleaved forest ecosystem and reconstruct a paleoclimate of southern Idaho that was much warmer and wetter during the mid-Miocene climatic optimum compared to today (Leopold and Denton, 1987; Mustoe and Leopold, 2014).

Idaho Group Sedimentation: Poison Creek and Chalk Hills formations

Following a hiatus after the deposition of the Payette Formation, the upper Miocene to Pliocene Idaho Group was deposited in a largely lacustrine environment (Lake Idaho; Cope, 1883). Although lake level dramatically fluctuated, had varying outlets, and was disconnected from the ocean at times (Wood and Clemens, 2002; Smith and Cossel, 2002), at its greatest extent Lake Idaho spanned several thousand km^2 (Kimmel, 1982; Viney et al., 2017). Variations in fish species present throughout the depositional history of ancient Lake Idaho serve as a proxy for changes in the size of the lake, changes in water composition, and the presence of an outlet to the ocean in the late Miocene-Pliocene (Smith and Cossel, 2002; Wood and Clemens, 2002). Abundant tephra were incorporated into the Idaho Group deposits and as time progressed, the amount of tuffaceous material declined. Much of the tephra likely originated to the east and southeast during extrusion of the Idavada volcanics (Tv on Fig. 1).

After the deposition of the Payette Formation, average global temperatures declined from ~16.5˚C at 13 Ma to ~10˚C at 9 Ma (Wolfe, 1995; Zachos et al., 2001; Buechler et al., 2007). By Pliocene time, the global temperatures had cooled, precipitation diminished, and the region became drier. The deciduous trees that were once common became rare. Dryland sage brush, salt brush, herbaceous flowering plants, and sparser conifers dominated the landscape. Regionally, the Cascade Range most likely reached current elevations in the early Pliocene following rapid uplift in the late Miocene (Mackin and Cary, 1965; Kohn et al., 2002; Reiners et al., 2002; Mitchell and Montgomery, 2006).

Mustoe and Leopold (2014) used fossil microfloras to estimate that the uplift of the Cascade Range was between ~8 to 6 Ma. They concluded that a 30 to 50% drop in mean annual precipitation occurred from ~12 Ma to ~3.4 Ma due to a combination of the rapid uplift and more globally widespread climate trends. Drier paleoclimatic conditions began during the deposition of the lower Idaho Group (Malde and Powers, 1962; Swirydczuk et al., 1982; Kimmel, 1982; Smith and Cossel, 2002; Wood and Clemens, 2002), as well as the 12 to 7 Ma Ellensburg Formation of central Washington (Smiley, 1963; Bingham and Grolier, 1966; Smith 1988a, 1988b; Smith et al., 1989), the 8 to 12 Ma Herron Group of central Oregon (Jijina et al., 2019), the 10.5 to 8.5 Ma Pickett Creek flora of Owyhee County, Idaho (Buechler et al., 2007), and the ~7 Ma Rattlesnake Formation of central Oregon (Dillhoff et al., 2009).

The Poison Creek Formation was named by Buwalda (1923) for a limited stratigraphic succession on the southern margin of the western Snake River Plain (Fig. 1). Using mammalian fossils and stratigraphic relationships, he suggested that the Poison Creek Formation was younger than the Payette Formation. In 1924, Buwalda reconsidered and suggested that the Poison Creek be considered as part of the upper section of the Payette Formation. In that same report, Buwalda suggested that the Payette Formation could also overlie the CRBG package. Although most early workers continued to suggest that there is an angular unconformity between the Payette Formation and the Poison Creek Formation, in 1931, Kirkham stated that he could not see it and suggested that there was instead a disconformable surface between the last CRBG flow and the overlying sediments.

Where Buwalda (1923) defined the type section of the Poison Creek Formation, along Poison Creek Grade (Fig. 1), the thickness of the entire section was less than 30 m . Malde and Powers (1962) accepted Buwalda’s designation and suggested that a thicker section (150 m occurred along Reynolds Creek southeast of Poison Creek. Near Homedale, they reported that the formation to be directly overlain by the younger Glenns Ferry Formation. Savage (1961) used the term Poison Creek Formation in the Emmett area but did not notice a striking difference from the overlying Idaho Group. Smith and Cossel (2002) used the Poison Creek designation for the deposits south of the Snake River Plain and suggest that unconformities bound the formation above and below. Their fish biostratigraphy indicates that the Poison Creek Formation was deposited during Clarendonian age (13.6 to 10.3 Ma) and could be as young as 9.0 Ma. In contrast, Wood and Clemens (2002) and Sander and Wood (2004) suggest that there are localized volcanic units with varying ages that cannot constrain the Poison Creek Formation. Wood and Clemens (2002) argue that the Poison Creek and Chalk Hills formation distinctions are not well defined and depending on the specific locality of the basin, either the Chalk Hills or the Poison Creek may overlie varying basalts, rhyolites, and the granitic Idaho batholith. Therefore, they regard the Poison Creek Formation as likely a facies within the Chalk Hills Formation associated with the basin margin during early rifting of the WSRP basin.

The Chalk Hills Formation was named by Malde and Powers (1962) for an area of badlands in the southeast part of the WSRP 22.5 km (14 miles) southwest of Bruneau (Fig. 1;). There, they described thin beds (1.5 to 3 m) of fine-grained sandstone and siltstone interbedded with silicic ash. Some have suggested that the lowermost Chalk Hills Formation may have been deposited in a series of lakes (Mustoe and Leopold, 2014; Viney et al., 2017). Kimmel (1982) suggested that the Chalk Hills lakes were interconnected, and Malde and Powers (1962) suggested that the Chalk Hills deposits have lateral continuity and were most likely deposited in a continuous shallow lake with intermittent stream inputs. Most likely, by the middle to upper Chalk Hills depositional time, one single enormous lake persisted throughout the WSRP.

Regionally the Chalk Hills Formation is thought to be about 8 to 9 Ma at the base (Kimmel, 1982; Armstrong, 1975; Smith and Cossel, 2002) and 5.9 to 5.5 Ma at the top (Kimmel, 1982; Smith et al., 1982; Perkins et al., 1998; Smith and Cossel, 2002; Wood and Clemens, 2002; Smith et al., 2013). Neither the maximum nor minimum ages are well constrained, and the formation may be bounded by variable unconformable surfaces in different parts of the basin (Wood, 2004). Although the cause of the regression (draining of the lake) at the end of the Chalk Hills Formation is unclear, Wood and Clemens (2002) suggested that the regressive lowstand is marked with a hiatus between 6 and 4 Ma.

Idaho Group Sedimentation: Glenns Ferry Formation

The Glenns Ferry Formation represents the last stage of ancient Lake Idaho (Figs. 2, 3, and 4), which was deposited as drying and cooling of the paleoclimate continued. The basal deposits of the Glenns Ferry Formation are separated from the Chalk Hills Formation by a low angle angular unconformity marking a hiatus that represents a period of regression in the lake and low water levels (Wood and Clemens, 2002). Depending on the length of the hiatus, deposition of the Glenns Ferry Formation began sometime between ~5.5 Ma to ~4 Ma (Malde, 1972; Kimmel, 1982; Smith et al., 1982; Perkins et al., 1998; Smith and Cossel, 2002; Wood and Clemens, 2002). Above the base, a time-transgressive oolitic marker bed (Malde and Powers, 1962; Swirydczuk et al., 1980) or laterally equivalent coarse sand is defined to the southeast near Emmett and Boise, Idaho (Wood and Clemens, 2002; Feeney et al., 2018). Locally, the oolite and coarse sandstone contains fish fossils (Swirydczuk et al., 1980; Kimmel, 1982). Oolite lenses occur discontinuously in sandy deposits around the margins of the western Snake River Plain. These are interpreted as a "bathtub ring" of transgressive beach deposits as Lake Idaho became an alkaline closed-lake basin near a relative highstand (Warner, 1975; Swirydczuk et al., 1979; Wood and Clemens, 2002; Wood, 2004). The last deposits of the Glenns Ferry Formation consist of the infilling of ancient Lake Idaho with a thick, laterally extensive sand unit. This sand was mapped in the Holland Gulch quadrangle by Forester and Wood (2012), who speculated that it may be equivalent to the Pierce Gulch Sand near Boise described by Wood and Clemens (2002), and Wood (2004).

The Glenns Ferry Formation was named from the type section west of Hagerman, Idaho (Malde and Powers, 1962; Fig. 1). Pliocene to Pleistocene in age, it has paleomagnetic ages of 3.79, 3.32, and 3.09 Ma near the Horse Quarry of the Hagerman Fossil Beds National Monument (Nelville et al., 1979; Mustoe and Leopold, 2014). The Glenns Ferry Formation is thought to be about 4.2 to 3.2 Ma to the east at Hagerman (Izett, 1981; Hart and Brueseke, 1999; Link et al., 2002) and as young as 1.5 to 1.67 Ma in the west near Caldwell (Repenning et al., 1995). A basalt that overlies the Glenns Ferry (Pickles Butte basalt) was dated using Ar-Ar methods at

1.67 Ma and indicates that ancient Lake Idaho drained by that time (Othberg, 1994; Wood and Clemens, 2002). No age control is present in the northern part of the WSRP where we have mapped, but an age of about 4 to 1.5 Ma is suspected (Fig. 2). The end of the ancient Lake Idaho highstand occurred after the Snake River drainage capture into the Columbia River drainage (between 2 and 3 Ma) at the southern end of Hells Canyon (Wheeler and Cook, 1954; Malde, 1991; Othberg, 1994; Smith et al., 2000; Wood and Clemens, 2002).

METHODS

Geologic mapping at 1:24,000 scale was conducted in 14 7.5' quadrangles. The maps depicted rock units exposed at the surface or underlying a thin cover of soil or colluvium; alluvial and man-made surficial deposits were also identified where they form significant mappable units. Eight of these maps are posted on the Idaho Geological Survey website (Feeney et al., 2014, 2016a, 2016b, 2018; Feeney and Phillips, 2016, 2018; Feeney and Schmidt, 2019; Garwood et al., 2014; Lewis et al., 2016) and the remainder are in preparation. Previous work in the Holland Gulch quadrangle (Forester and Wood, 2012) and regional mapping and well analysis by the second author (Spencer Wood) inform our current efforts. Field work was augmented with whole-rock XRF geochemical analyses of volcanic rocks at Franklin and Marshall College and the results reported on the published maps.

Felsic volcanic units were targeted for U-Pb zircon dating in order to provide age constraints for the sedimentary unitsAll sample preparation and analytical measurements were performed in the Isotope Geology Laboratory at Boise State University Table 1). Zircon concentrates were obtained via crushing and standard density and magnetic separation techniques and annealed in a muffle furnace at 900º C for 60 hours in quartz crucibles to anneal minor radiation damage; annealing enhances cathodoluminescence (CL) emission (Nasdala et al., 2002), promotes more reproducible interelement fractionation during laser ablation (Allen and Campbell, 2012), and prepares the crystals for subsequent chemical abrasion (Mattinson, 2005). Following annealing, individual grains were hand-picked and mounted, polished, and imaged by cathodoluminence (CL) on a scanning electron microscope. For some samples, the polished zircons were then analyzed by laser ablation – inductively coupled plasma mass spectrometry (LA-ICPMS) using a New Wave Research UP-213 Nd:YAG UV (213) laser ablation system coupled to a ThermoElectron X-Series II quadrupole mass spectrometer following methods described in Macdonald et al. (2018). Based on LA-ICPMS $^{206}Pb/^{238}U$ ages, elemental data, and CL zoning patterns, subsets of zircons from each sample were plucked from the epoxy and subjected to a modified version of the chemical abrasion method of Mattinson (2005), whereby single crystal fragments plucked from grain mounts were individually abraded in a single step with concentrated HF at 190°C for 12 hours.

Chemical abrasion isotope dilution thermal ionization mass spectrometry (CA-IDTIMS) analyses were performed on an IsotopX Isoprobe-T multicollector mass spectrometer following procedures described in detail in Macdonald et al. (2018). U-Pb dates and uncertainties for each analysis were calculated using the algorithms of Schmitz and Schoene (2007) and the U decay constants of Jaffey et al. (1971). All geological ages are interpreted from the weighted means of multiple single crystal $^{206}Pb/^{238}U$ dates and the errors for these ages are reported at the 95% confidence interval in the form of ±X(Y)[Z], where X is the internal standard deviation multiplied by the Student's t-distribution multiplier for a two-tailed 95% critical interval and n-1 degrees of freedom, and by the square root of the reduced chi-squared parameter (or mean squared weighted deviation (MSWD); Wendt and Carl, 1991), when necessary to accommodate unknown sources of overdispersion, Y is this analytical uncertainty combined with the uncertainty in the mixed U-Pb EARTHTIME 535 tracer calibration (0.03%; Condon et al., 2015; McLean et al., 2015), and Z convolves the ^{238}U decay constant uncertainty (0.018%; Jaffey et al., 1971) with the uncertainty in Y. The full isotopic data and interpreted ages are presented in Table 1.

Palynomorphs were extracted and analyzed from surface samples and well cuttings from five of the initial Bridge and Paramax Resources Ltd. exploratory wells. Samples were processed by Global Geolab Limited in Medicine Hat, Alberta. Five grams of each sample were washed, crushed, and processed using hydrochloric acid and hydrofluoric acid maceration, oxidation of organics, sieving, and separation of the clay grains. The palynomorph slides were examined and photographed under 1000x power under a transmitted light microscope. Depths of sampled well cuttings are indicated in Figure 5. Index palynomorphs were then identified stratigraphically to show the reduction or disappearance of warmer-climate trees and an increase in cooler-climate plants as an indicator of cooling, attributed to the presence of the Mid-Miocene Climatic Optimum temperatures and cooling thereafter. The presence of grains is a function of 1) climate; 2) proximity of the plant to the deposition site; 3) type of dispersal method for the grain (zoophyllis, anemophilous, etc); 4) number of grains a plant produces in a year; and 5) preservation quality. These factors were considered in the analysis.

More than fifty distinct palynomorphs were identified (Table 2). Each of the surface samples aided in the determination of palynomorph biozones. These biozones are defined using fossil assemblages as well as index fossil grains. Surface samples of nearby outcrops that have been radiometrically dated were instrumental in providing time constraints for the floral assemblages that define each of the formations. Plant macrofossils from surface outcrops were also described and are compared here to determine vegetation type in each formation. Results are given in Table 3, select grains are shown graphically in Figure 6, and identified grains from the 5 wells are provided in Table 4.

ANALYSIS AND DISCUSSION

Payette Formation

Our mapping north of the WSRP indicates that the definition of the Payette Formation needs revision. The formation consists of mudstone with lesser amounts of weakly consolidated to highly silicified sandstone to granule conglomerate (Fig. 6). Based on the abundant quartz, feldspar, biotite, and muscovite the most likely provenance of the sediments is the nearby Idaho batholith. Ash beds are common and can occur as thin synchronous beds or thick reworked deposits. Diatoms are locally present in the finer grained beds. Mudstones are brown and green, have a high bentonite content, and weather to a “badlands” topography and appearance. The brown and reddish mudstones are interpreted as paleosols due to their high clay content and local occurrence of rootlets. As noted previously, Lindgren (1898) estimated the thickness of the Payette Formation in Horseshoe Bend vicinity to be ~300 to 366 m. In the Alkali Creek area, northwest of Emmett, Idaho the maximum thickness is estimated at ~700 m based on our unpublished mapping (Love et al., 2021 in prep; Lewis et al., 2021 in prep). The formation thins to the southeast toward Emmett by an erosional contact (Fig. 3).

Originally the Payette Formation was thought to be deposited mostly in a large lacustrine setting (Lindgren, 1898; Buwalda, 1924). Based on the uncertainty of the assignment of the Payette Formation and overlying Idaho Group sedimentary packages, it appears that this designation was perhaps a result of some of the Lake Idaho sediments being included within the Payette Formation (Kirkham, 1931). We interpret the dominant depositional environment for the Payette Formation in the study area to be fluvial and localized quiet-water back swamp deposits, with lesser lacustrine deposits. The fluvial deposits are characterized by coarse to very coarse arkose to quartz arenite to fine conglomerate. Finer lacustrine intervals are thick- to thin-bedded tuffaceous mudstone and volcanic ash deposits. These locally are fossil-bearing (infrequent thin beds of ostracod and plant remains), which act as distinct local marker beds (Breedlovestrout et al., 2017). Regional marker beds are volcanic ashes with specific geochemical signatures that can be mapped laterally (Nash and Perkins, 2012). Dip changes indicate an unconformity between the Payette Formation and the overlying Lake Idaho sedimentation. We are uncertain about the duration of the hiatus between the Payette Formation and Idaho Group and whether it varies from place to place in the WSRP basin.

Our mapping shows that the Payette Formation locally contains higher concentrations of organic matter than the overlying Chalk Hills and Glenns Ferry formations, but it is still sparse in surface exposures. Total organic content may be greater in the subsurface deeper in the basin and a potential contributor to the Willow and Hamilton hydrocarbon fields to the west in the Sheep Ridge and Birding Island quadrangles (Fig. 3). In addition to higher organic matter content, paleosols characterized by reddish brown, clay-rich zones developed locally in the Payette Formation are indicative of the warmer paleoclimate of the mid-Miocene climatic optimum. These observations are consistent with the bulk of Payette Formation having been deposited during that time.

Two high precision U-Pb zircon age determinations from the Alkali Creek area north of Emmett provide important constraints on the age of Payette Formation sedimentation (Table 1; Fig. 9; Feeney et al., 2017). The oldest age (sample 16DF438) is from the rhyolite of Indian Creek in the southern part of the Paddock Valley Reservoir quadrangle (Figs. 3 and 4). This rhyolite is within the lower part of the Payette Formation. It is characterized by <5% of phenocrysts of plagioclase up to 2 mm in length in a groundmass of devitrified glass. We dated this rhyolite at 16.395 ± 0.009 Ma on the basis of nine concordant and equivalent single zircon U-Pb analyses (Fig. 9). Overlying the rhyolite of Indian Creek is 30 m of silty claystone, followed by a lapilli-rich unwelded tuff (Fig. 6). Capping the lapilli tuff is a densely welded tuff 1 to 5 m thick. It contains plagioclase and sparse quartz phenocrysts and contains glass that compositionally (Barbara Nash, written comm., 2018) is trachydacite. The lapilli contain a few percent plagioclase and the composition of the glass is 66.9-69.4 percent SiO_2 and 8.1-9.4 percent total Na_2O+K_2O (Barbara Nash, written comm., 2018). Our new U-Pb zircon geochronology dates this lapilli tuff at 15.882 ± 0.020 Ma (sample 15DF415, Table 1; Feeney et al., 2017), on the basis of four concordant and equivalent single zircons. The age of this prominent lapilli tuff marker bed is equivalent within analytical error to the $^{40}Ar/^{39}Ar$ age of 15.91 ± 0.05 Ma (recalculated to an age of 28.21 Ma for the Fish Canyon sanidine monitor standard) for the Tuff of Leslie Gulch in the nearby Rooster Comb Caldera and Lake Owyhee Volcanic Field of eastern Oregon, reported by Benson and Mahood (2016). This correlation allows us to equate this part of the Payette Formation with the lower lacustrine strata of the Sucker Creek Formation to the south. Higher still (roughly 500 m above the lapilli ash but this area is complicated by faulting) is an ostracod-bearing ash layer whose composition matches that of the 'Obliterator ash' from the Succor Creek area just west of the Idaho border (ash a2 of Lawrence, 1988, and ash III of Downing and Swisher, 1993, dated at 14.93 ± 0.08 Ma using Ar-Ar methods). These ages and correlations indicate that the enclosing sedimentary strata that we assign to the Payette Formation were deposited between 16.39 and 14.93 Ma. Thus, the earlier definition of the Payette Formation that only includes sediments interbedded within the CRBG volcanic flows by Kirkham (1931) needs to be revised. Clearly the sedimentary section in some localities above the uppermost volcanic flows is older and Payette Formation in age.

Palynomorphs from 13 surface localities (Table 3) indicate that during the deposition of the Payette Formation, common conifers in the forests included *Abies, Picea, Taxus, Pinus, Tsuga, Pseudotsuga/Larix*, *Cedrus*, and *Taxodium/*Cuppressaceae (see Table 2 for common names). Most likely, these conifers inhabited upland environments and were transported. Deciduous trees and shrubs included *Acer*, *Alnus, Betula, Carya*, *Castenea*, *Eleagnus*, *Liquidambar, Ostrya, Platanus*, *Pterocarya, Juglans*, *Quercus*, *Tillia*, *Nyssa*, and *Ulmus/Zelkova*. Herbaceous and other small plants included Caryophyllaceae and *Isoetes*.

Less common grains included Chenopodiaceae/Amaranthaceae, *Fagus*, *Fraxinus*, Poaceae/Graminae, *Nymphaea*, Ericaceae, and *Salix*. While some of these species lived in and along bodies of water (cypress and water lilies), others grew in the flood plain environments of the lowlands and slopes. Similar modern forests that contain these genera are from eastern Asia and eastern North America (Dillhoff et al., 2009). Cypress swamps today occur in the Mississippi Valley near the Gulf of Mexico. Other less diagnostic grains not mentioned here are included in Table 4.

Three surface localities also contained plant macrofossils (leaves, reproductive structures, and branches) in the Payette Formation (Fig 3, Table 3). Identified leaves and needles are from *Metasequoia, Cercidophyllum, Glyptostrobus, Chamaecyparis,* Lauraceae, *Platanus, Taxodium, Sassafras, Lithocarpus, Quercus, Sequoia, Equisetum,* and possibly *Castenea* and *Betula.* One of the localities south of Paddock Valley Reservoir is one of the few sites where *Sequoia* and *Metasequoia* overlap in the fossil record (Patrick Fields, 2019, personal comm.) and it is rare to find them in the same stratigraphic sequence. Although some of these genera do not have readily preserved palynomorphs, this assemblage aligns with the pollen grain assemblages mentioned above.

As mentioned previously, the Payette Formation is the only sedimentary formation with observed lignitic and sub-bituminous coal interbeds and is the main hydrocarbon source in the basin. The mid-Miocene climatic optimum provided a warm environment conductive of abundant, diverse plant growth and high rates of plant death and accumulation. Several centimeters to 1 m thick subbituminous coal has been observed in other Payette Formation localities near Horseshoe Bend (Bowen, 1913). In the mapping area, a lignite bed occurs along Indian Creek (Fig 3) and records macroflora of *Metasequoia* and possible *Quercus* as well as small pieces of wood. Interspersed with sedimentary interbeds, this section contains ~1.5 m of coal and other organic-rich rock. Nearby dating indicates that this lignite would be slightly older than the 16.4 Ma rhyolite dated nearby (sample 16DF438, Table 1).

The Mascall Formation of central Oregon was deposited during a similar time to the Payette Formation (16-12 Ma; Bestland et al., 2008). Dillhoff et al., (2009) and Chaney and Axelrod (1959) reported fifteen common species that occur in the Mascall formation; these include different species of *Taxodium, Quercus, Carya, Quercus, Platanus, Acer, Metasequoia, Ginkgo, Ulmus, Cedrela, Ulmus,* and *Betula*. Extensive work has also been done on the age-equivalent Latah Formation of eastern Washington and northern Idaho. Although Poaceae/Gramineae, *Eleagnus,* and *Isoetes* grains are infrequent, the other palynomorphs mentioned above are common (Knowlton, 1926; Smiley et al., 1975a). The genera in both the Latah and Mascall formations above were common during the mid-Miocene and have commonalities to the Payette Formation flora and the palynomorphs analyzed. This also helps confirm and establish the lower age of the Payette Formation at about 17 to 15 Ma during the mid-Miocene climatic optimum based on the presence of *Liquidambar*. The minimum age for the Payette is still uncertain.

The results of our new geochronology, mapping, and biostratigraphy indicate that the Payette Formation is interbedded with, but also locally overlies the middle Miocene volcanic flows (Figs. 2, 3, and 4). As discussed previously, there have been different definitions of the Payette Formation—whether it is only interbedded with or whether it is interbedded with and overlies the

CRBG and Weiser volcanics (Lindgren, 1898; Kirkham, 1931). We redefine it here as the sedimentary deposition that overlies and is interbedded with the Columbia River Basalt Group and Weiser Volcanics, spanning the mid-Miocene climatic optimum.

Poison Creek and Chalk Hills formations

Northwest of Emmett, we mapped only the Payette Formation and overlying deposits that we ascribe to the Chalk Hills Formation and were not able to distinguish a mappable unit that could be called the Poison Creek Formation. If present in this area, we consider the Poison Creek Formation to be a member in the initial (possibly discontinuous) asymmetric basin of Lake Idaho within the lower Chalk Hills Formation. Thus, our stratigraphic succession is Payette Formation upward into the Chalk Hills Formation with a hiatus in between (Figs. 2 and 4).

Zircons from a lapilli tuff layer near base of the sedimentary section along Anderson Creek (Fig. 3) to the east in the neighboring Montour quadrangle yield a range of U-Pb ages, indicating abundant detrital reworking (sample 14RL065, Table 1; Lewis et al., 2016). We thus interpret a maximum depositional age of 9.896 ± 0.022 Ma from the youngest single zircon analysis, for both this tuff and the hosting strata that we assign to the Chalk Hills Formation. Little, if any, Payette Formation is preserved in this area.

A high-precision U-Pb age of 9.041 ± 0.016 Ma was determined from eight concordant and equivalent single zircon dates in a lapilli-bearing interval of a 5-m-thick light-gray ash and lapilli marker bed (sample 15RL014, Table 1; Fig. 9; Feeney et al., 2018) from east of Emmett (Fig. 3).

The lapilli contain about 2 percent quartz and 1 percent sanidine along with obsidian fragments in a rhyolitic matrix (Feeney et al., 2018).

A 10 to 20 m thick tephra-rich interval is exposed in Haw Creek north of Emmett (Fig. 3; Feeney et al., 2018). The base of this interval contains large white pumice blocks as much as 15 cm in diameter (Fig. 7, and zircons from these pumice blocks yield a U-Pb age of 9.005 ± 0.0015 Ma on the basis of six concordant and equivalent crystals (sample 15RL015a, Table 1; Feeney et al., 2018). The pumice contains about 3 percent sanidine phenocrysts (Fig 7.). Whole-rock XRF reported by Feeney et al. (2018) indicate a rhyolitic composition. This sample came from a section near the top of the Chalk Hills Formation about 100 m below the base of the Glenns Ferry Formation.

These ages from the Emmett area that range from <9.9 to 9.0 Ma are important from the standpoint of formation designation. Earlier workers who dated the lowermost Idaho Group suggest that these dates would place these units in the Poison Creek Formation whereas here, we would incorporate it as a facies into the lowermost Chalk Hills Formation. Additional mapping and geochronologic work are required to understand the age relationship between outcrops to the south at Poison Creek and in the type Chalk Hills to the southeast (Malde and Powers, 1962), and how those relate to exposures mapped here as Chalk Hills Formation. Both Mustoe and Leopold (2014) and Mapel and Hail (1959) combined data for the Poison Creek and the Chalk Hills Formations because they are both very close in age (early Barstovian) and have similar depositional setting.

We have also dated a pumice-rich interval from Sulfur Gulch in the Hog Cove Butte quadrangle (Fig. 3; Fig. 9; Love et al., 2021, in prep.). The interval is a light-gray, non-welded to weakly welded tuff with conspicuous pumice clasts 5 to 10 cm in diameter. The pumice contains euhedral 0.5 to 3 mm sanidine and quartz phenocrysts, and zircons with a U-Pb age of 7.776 ± 0.013 Ma (sample 16RLB014, Fig. 9; Table 1). This interval forms an important marker bed in the eastern to central part of the quadrangle and is roughly 70 m above the base of the Chalk Hills Formation, suggesting that lower part of the Chalk Hills Formation present at Anderson Creek is missing here. Whole-rock XRF analyses indicate a rhyolitic composition. Its age affirms its correlation to the Chalk Hills Formation on the south side of the plain (Kimmel, 1982; Smith et al., 1982; Perkins et al., 1998; Smith and Cossel, 2002).

Our mapping north of the western Snake River Plain shows that the Chalk Hills Formation occurs as unconsolidated to moderately consolidated tuffaceous siltstone, tuffaceous claystone, very coarse to fine sandstone, and white to red arkosic fine conglomerate interspersed with ash and tuffaceous pyroclastic intervals (Fig. 7). Its stratigraphic architecture comprises of massive 12 to 60 m units with “chalky” tuffaceous clay-rich intervals and more isolated iron-stained sandstone beds. The base is defined by a thick sand interval in lower Alkali Creek. The sandstone is arkosic, fine to coarse grained and contains subangular to subrounded grains of quartz, potassium feldspar, plagioclase feldspar and, in places, trace amounts of biotite, muscovite, amphibole, lithics, obsidian, and white volcanic ash. The top of the formation is poorly defined but lies above the uppermost thick interval of tuffaceous mudstone. The thickness is estimated to be ~300 to 520 m.

The Chalk Hills Formation is lighter in color and more massive than the underlying Payette Formation. Exposed soils overlying the Chalk Hills Formation locally have a lower clay content than the Payette Formation resulting in limited desiccation cracks in soils. Dips of the Chalk Hills Formation are less steep than the underlying Payette Formation strata. Organic matter is even rarer than that found in the Payette Formation.

These deposits are interpreted as lacustrine with many silicic volcanic ash beds based on the parallel-laminated, fine-grained tuffaceous deposits and the presence of diatoms. A minor fluvial to subaerial channel component is suggested by 2D seismic lines and are present in isolated compartmentalized beds. Lowermost deposits may represent a shallow disconnected lake with close-to-the source fluvial, deltaic, and volcanic inputs. As time progressed, the lake level apparently rose, resulting in more massive, laterally continuous, highly tuffaceous lacustrine deposits. The top locally is well documented by a 10-35 m thick reddish brown paleosol developed above the dated 9.041 Ma ash in the NE Emmett quadrangle (Feeney et al., 2015).

The presence of floral assemblages in outcrop samples in combination with index fossil palynomorphs for the Chalk Hills Formation aid in the correlation. The palynomorph assemblage from the Chalk Hills Formation time included similar genera as the Payette Formation with the addition of *Cathaya*, *Ephedra*, *Sarcobatus*, Rosaceae, and Onagraceae. More abundant *Pinus, Cedrus,* Caryophyllaceae, *Asteraceae, Artemesia,* and Chenopodiaceae also occur, while *Liquidambar* disappeared here and regionally after the mid-Miocene climatic optimum. In particular, *Ephedra, Sarcobatus, Asteraceae*, and *Artemesia* represent the onset of drier vegetation. These plants represent the changing of paleoclimate from humid and warm to cool and dry.

The nearby Pickett Creek flora of Owyhee County, Idaho on the south side of the WSRP are similar in age to the Chalk Hills Formation. Chemical analyses of two ash samples from Pickett Creek suggest an age of 8.5-10.5 Ma (Buechler et al., 2007). Abundant palynomorphs listed for the Pickett Creek Flora are *Pinus* and *Quercus*, while more rare grains that also indicate a slightly drier paleoclimate are Asteraceae, Onagraceae, and Chenopodiaceae/Amaranthaceae. The Musselshell Creek flora in northern Idaho is either slightly older than or age-correlative to the lowermost Chalk Hills Formation. Ages of that flora span 12.5-10.5 (Baghai and Jorstad, 1995). Ma. In this flora, a similar trend exists: the deciduous-hardwood flora common also to the Payette Formation was replaced by drier, more temperate forests; *Taxodium*, *Sequoia*, and *Metasequioa* are replaced by *Abies*, *Picea*, and *Pinus* (Baghai and Jorstad, 1995). Viney et al. (2017) documented at least fifteen angiosperm and gymnosperm types in the Bruneau Woodpile of the Chalk Hills Formation south of Bruneau (Fig. 1). This specific site was dated at ca. 6.85 Ma. Macrofossils included gynmosperms Cuppressaceae and *Pinus*, and angiosperms included cf. *Berberis,* Fabaceae, *Quercus, Carya, Salix, Acer,* and *Ulmus.* Except for the *Berberis* and Fabaceae, the Bruneau Woodpile macrofossils (Viney et al., 2017) are comparable to the palynomorphs presented here and represent a subset of the drier forests of the late Miocene.

Glenns Ferry Formation

The Glenns Ferry Formation north of the WSRP consists of unconsolidated to moderately consolidated siltstone, claystone, very coarse to fine arkosic sandstone, and fine conglomerate interspersed with minor amounts of admixed fine tuffaceous material (Fig. 8). Finer material is a well-bedded finely laminated siltstone to claystone with local diatoms. Arkosic deposits consist of medium gray to tan, fine to coarse, subangular to subrounded grains of quartz, potassium feldspar, plagioclase feldspar, biotite, and muscovite. Minor volcanic lithic fragments consist of brown glass, basalt, and possibly rhyolite. North of the WSRP, the maximum thickness may be as much as 915 m. In the central and southern WSRP, the Glenns Ferry Formation may be as thick as 540 m (Wood, 1994).

The Glenns Ferry Formation differs from the underlying Chalk Hills Formation in that it contains less ash and less mudstone, less clay overall, and is darker (brown to tan) and more clearly layered when viewed from a distance (or in Google Earth images where unit typically has a distinct maroon color). Stratigraphic architecture and appearance is a tan to maroon thinly-bedded 30 cm to 3 m aggradational sequence with local thicker 1.5 to 15 m sandstone beds. Deposits are interpreted as partly lacustrine based on an abundance of parallel laminae and fine grain size found regionally; a fluvial and deltaic component consists of interbedded siltstone to fine to coarse sandstone (Wood and Clemens, 2002). Mud cracked surface soils are rare.

A general cooling and drying trend continued from the Miocene to the Pliocene in Idaho. More arid, sagebrush-woodland and grassland steppe environment with smaller herbaceous plants and an increase of Asteraceae characterized the Pliocene Glenns Ferry Formation (Leopold and Denton, 1987; Mustoe and Leopold, 2014). The deciduous trees that were regionally still abundant during the late Miocene became rare (*Carya, Quercus, Acer, Juglans*, and *Ulmus*; Mustoe and Leopold, 2014). More frequent *Juniperus*, Poaceae/Gramineae, *Artemesia*, Chenopodiaceae, Asteraceae, and *Sarcobatus* occurred which is consistent with the grassy-steppe environment described in other studies (Leopold and Denton, 1987; Mustoe and Leopold, 2014; Viney et al., 2017). It is important to point out that *Pterocarya* is also absent (but it was in high abundance during the Chalk Hills depositional time). The palynomorphs observed for the Glenns Ferry Formation in this study were also reported for the Horse Quarry near Hagerman Fossil Beds National Monument in Mustoe and Leopold (2104). The vegetation in the Pliocene in the basin is comparable to the vegetation in Boise, Idaho today. Desert vegetation and grasses predominate whereas larger coniferous trees grew in the uplands near water drainages.

Composite Sections: Biostratigraphy and lithology of well cuttings

The following index palynomorph grains representing the change in vegetation, and therefore climate, are identified from oil and gas well cuttings and surface deposits and are useful as biostratigraphic indicators: *Juniperus, Poaceae/Gramineae, Artemisia, Asteraceae, Pterocarya,* and *Liquidambar* (Fig. 5). The reduction or disappearance of some warmer-climate deciduous trees (*Platanus, Liquidambar,* and *Pterocarya)* is an indicator of cooling. The presence of grasses alongside sagebrush and saltbrush also indicates a general cooling. Examination of the palynomorphs is important for determining microfossil biozones in the subsurface. These biozones are defined using fossil assemblages as well as index fossil grains. The well cuttings from the first five wells that were drilled by Bridge Resources Corp. and Paramax Resources Ltd. are used in this biostratigraphic analysis (Fig. 5).

Two intervals in Island Capital 1-19, at 1073 and 1234 m, contained the biostratigraphically useful index fossil grain *Liquidambar*, which disappeared from the fossil record as paleoclimate became cooler and drier after the mid-Miocene climatic optimum. Along with the other grains provided in Table 4, these assemblages suggest deposition during the Payette Formation time. What does not occur in Island Capital 1-19 below 1073 m are the grassy, herbaceous desert steppe flora of the late Miocene and early Pliocene. The high abundancy of deciduous trees largely disappeared by the early Pliocene. The presence of the semi-arid steppe indicators alongside some of the deciduous trees suggests that the upper layers in Island Capital 1-19 (depths 97 to 512 m) were deposited in the late Miocene Chalk Hills Formation time. We had independently mapped the surface deposits at the Island Capital 1-19 well head as Chalk Hills Formation, which is consistent with this assessment (Fig. 3; Lewis et al., 2021, in press). The Glenns Ferry crops out slightly to the north and caps the hillsides above the well. Presumably, the surface exposures are representative of the upper Chalk Hills Formation.

Liquidambar occurs along with a diverse assemblage that indicates a mixture of deciduous and coniferous forests from 631 to 509 m in Schwarz 1-10. There is a gradual progression in the changing flora, between the mid-Miocene flora of the Payette Formation and the late-Miocene flora of the Chalk Hills Formation, and although *Liquidambar* does not occur between 473 to 405 m, we are also designating these depths as Payette Formation due to nearby surface mapping (Love et al., 2021, in prep.). The well was drilled in the lowermost Chalk Hills and our interpretation is that the Payette Formation should be close to the surface. At the depth of 265 to 268 m in Schwarz 1-10, typical Chalk Hills flora occur. Fewer deciduous trees occur, and the drier desert-steppe plants are more abundant. At 40 to 43 m the assemblage is characteristic of the Pliocene Glenns Ferry depositional time, but it may also represent post Glenns Ferry Formation deposition in the modern floodplain. Quaternary gravels are present at the well head and would have similar characteristic palynomorphs, making it difficult to determine which is represented at this interval. Based on surface mapping, we favor that the Quaternary gravels are represented. Thus, much of the upper Chalk Hills Formation and all of the Glenns Ferry Formation have been eroded and are absent.

The ML Investments 1-10 well is in the center of the Willow Field (Figs. 3 and 4) and its well head is at the site of the High Mesa Holdings separation facility for the produced hydrocarbons of nearby wells. The two bottommost zones, at 1182 to 1494 m are designated as Payette Formation here. Although the 1494 m interval did not contain *Liquidambar,* the grain is present at 1182 m which makes everything beneath it older. Barton (2019) places the contact lower based on seismic reflection data, but unless the Liquidambar pollen reported here is reworked, we prefer the contact placement shown in Figures 4 and 9. As stated previously, the presence of grains is a function of 1) climate; 2) proximity of the plant to the deposition site; 3) type of dispersal method for the grain4) number of grains a plant produces in a year; and 5) preservation quality. The absence of *Liquidambar* in the lowermost zone could reflect any one of these functions and is not diagnostic of a biostratigraphic age.

The interval of 856 to 859 m in ML Investments 1-10 contained a degraded grain that is tentatively identified as *Liquidambar*. It is interpreted here as a reworked grain. At the depth of 591 to 594 m, typical Chalk Hills palynoflora occur. Between 405 to 408 m grains that represent the slow transition between the coniferous forests of the Chalk Hills Formation and the arid deserts of the Glenns Ferry Formation are present. It is unclear if this sample represents the lowermost Glenns Ferry Formation or uppermost Chalk Hills Formation. Either way, it was most likely deposited sometime between 4 and 6 Ma, either preceding or following the potential hiatus between the two formations. Lastly, the sample that was analyzed for the depth 100 to 103 m has typical Glenns Ferry Formation grains.

Cuttings from two wells in the Hamilton Field to the south (Espino 1-2 and State 1-17; Fig. 3) are also examined. The bottom two intervals in Espino 1-2, 1173 and 966 m are designated as Payette Formation here based on unmistakable *Liquidambar* pollen grains in the 966 m interval. Similar to the ML Investments 1-10 well, the lower interval (1173 m) did not contain *Liquidambar*. The sample taken at a depth of 500 to 503 m contained a palynomorph assemblage that reflects a drying climate. Given the fossil assemblage as a whole, we designate this interval as being deposited during the Chalk Hills time. The uppermost intervals sampled at 354 and 253 m are interpreted as being deposited during the Glenns Ferry time. There are differences in palynomorphs between the two intervals, but both contain copious grassland-desert steppe floras. Two notable grains that become absent in the fossil record in both samples are *Pterocarya* and *Platanus.* Both of these grains are common in the Chalk Hills and Payette flora and become much less common in the Glenns Ferry flora.

Lastly, results from the State 1-17 are consistent with the findings at depth in the other wells. Interval 1289 to 1292 m contained a single degraded *Liquidambar* grain, and the depth of 1097 to 1100 m contained an indisputable *Liquidambar* grain, placing both intervals in the Payette

Formation. Sample 411 to 414 m is designated as Chalk Hills Formation due to the presence of a combination of desert and conifer forest flora. Lastly, we designate the interval between 192 to 195 m as Glenns Ferry Formation based on the desert palynomorphs present.

FURTHER IMPLICATIONS

Implications for Producing Zones and Reservoir Thickness

After the palynomorph biozones were defined and correlation from well to well was completed, the composite sections of each formation can be interpreted from subsurface logs (Fig 10). In the Willow and Hamilton fields, the subsurface Payette Formation consists of volcanic rocks and intrusive sills interlayered with mudstone, siltstone, and sandstone. The volcanic rocks are mostly basaltic in composition based on gamma ray values 25-50 gAPI. Although the wells did not drill through the entire interbedded Payette Formation and volcanic section and a full section has yet to be recorded, the electronic logs indicate that there is a minimum of 365 m of sedimentary interbedded material between the volcanic intervals. Above the uppermost volcanic unit, palynology data and surface mapping suggest that between 460 to 760 m of sedimentary rocks should also be included within the Payette Formation in the Willow Field. Total minimum thickness of the Payette Formation is thus ~900 m (see ML Investments 1-10). The producing sand reservoirs in the Willow Field (termed the Willow, DJS, and other unnamed sands by Bridge Resources, Paramax Resources, and Alta Mesa) occur ~150 to 300 m above the top of the first major volcanic unit encountered in the subsurface and are perforated in the Payette

Formation. Depths of these producing zones are between ~960 and 1600 m although the majority are between 1158 and 1494 m. Thicknesses of these reservoirs are between 15 and 45 m.

Using the above palynomorph analysis, and the stratigraphic architecture and lithologies present in the gamma ray and resistivity petrophysical logs, formation tops are extrapolated from the wells with biostratigraphic control to other wells in the Willow and Hamilton fields without biostratigraphic control (Fig. 10). Fining upward, coarsening upward, and aggradational packages are also considered. Also, flooding surfaces and maximum flooding surfaces provided chronostratigraphic markers. Here, horizons are correlated across the fields. Using those correlations, estimated locations of each of the formation tops are indicated at depth.

The Chalk Hills Formation is a largely tuffaceous siltstone and mudstone with several discontinuous sand units. One of these sand units provided the first hydrocarbons that were produced in Idaho in the State 1-17 well between the depth of 563 to 610 m (termed the Hamilton or upper sands). This was the only producing interval in the Hamilton field. The thickness of the Chalk Hills Formation in the producing field is ~300 to 460 m based on the palynomorph analysis. The sandstones in the Chalk Hills Formation act as a hydrocarbon reservoir but sufficient organic material has not been observed to suggest that they contributed as a source of the hydrocarbons. The sands of the Chalk Hills Formation are most likely deltaic and either pinch out to the southwest in deeper parts of the basin or form of isolated to amalgamated channel sands in the center of the basin. The bentonitic tuffaceous mudstones, which dominate the formation, most likely act as a sealing facies for the oil, liquid condensate, and natural gas.

The oil and gas operating companies usually set the conductor casing just after a sandy unit that represents the bottommost Glenns Ferry Formation. This represents either the lowstand of ancient Lake Idaho and subsequent rapid transgression or a deltaic sequence during the highstand of the lake. Because much of the Glenns Ferry in the Willow Field is eroded away at the surface, a maximum thickness cannot be estimated. In the well logs, we see the lower 150 to 300 m of the formation which are lacustrine stacked density flow sands (Wood, 1994). The bottommost interval of the Glenns Ferry Formation consists of sandstone interbedded with siltstone. Sand units are as much as 122 m thick. From surface mapping, we describe the remainder of the Glenns Ferry as siltstone and coarse sandstone units interbedded with mudstone.

The Glenns Ferry Formation most likely acts as the overburden to the petroleum system in the subsurface. The basal Glenns Ferry Formation is thought to have formed as a transgressing sequence (Wood and Clemens, 2002). It is important to note the influence that this would have on the petroleum play elements in the basin. Deltaic reservoir sands would have stayed close to the lake margins and significant reservoir beds would not have made it to the center of the basin. This would create a scenario where large sandy units of the underlying Payette and lower Chalk Hills formations would be overlain by large deposits of sealing mudstone facies. The character and thickness of any sealing facies of the Glenns Ferry Formation north of the WSRP is uncertain., Some has been removed by erosion and the upper part was not geophysically logged.

To summarize, a Wheeler Diagram was created from Weiser, ID to Mountain Home, ID (Fig.11). The Payette Formation is restricted to the area near Weiser and Horseshoe Bend, ID and does not extend as far as Mountain Home. It is interbedded and overlies the Columbia River

Basalt Group and Weiser volcanics. Figure 11 shows the facies changes within the study area through geological time and space. Although Wheeler diagrams commonly show eustatic changes, this figure shows lake level changes and local accommodation versus exposure over time.

Implications for timing and petroleum play elements

The placement of the 150 to 300 m thick sedimentary section above the uppermost volcanic unit is important when defining properties of the petroleum play in the basin. The majority of the producing zones are in the Payette Formation between 1158 and 1494 m measured depth (MD; Fig. 10). With this knowledge, surface analogues for reservoir properties, type of organic matter (source), and maturation/migration timing can begin to be inferred. For the hydrocarbons to mature from plant material and become captured in the reservoir, the reservoir facies had to be deposited, buried at sufficient temperature and pressure at depth for maturity to take place, a migration conduit had to form (structural or stratigraphic), and then the hydrocarbons could migrate into the reservoir facies. To keep the reservoir in the ground, either a sealing or capping facies and trapping mechanisms had to be in place and further burial had to cease before the hydrocarbons became over-mature into dry gas or barren material.

With our new WSRP chronostratigraphic constraints, we know the approximate age of the Payette Formation (~17-12 Ma). This was the time when organic source material was likely to have been deposited. With rare exceptions, however, organic sections have not been located by our mapping. Two wells in the Willow field logged ~30 m of black shale with coaly cleats in the 1200-1700 m deep section, and these appear to be the most promising source rocks to data.

Fluvial, deltaic, back swamp, and smaller restricted lacustrine depositional environments of the Payette Formation provided sedimentary packages with thick reservoir sands that may have been interbedded with appropriate source material during a thermal optimum climatic interval. At around 12 Ma, the Payette was likely exposed and partly eroded before the Chalk Hills Formation was deposited.

Burial of the source rocks began during the onset of ancient Lake Idaho and the deposition of the Chalk Hills Formation. From the new 9.04, 9.01, and 7.78 Ma dates, we suspect that this burial began around 10-11 Ma. Deposition continued until ~5 to 6 Ma when another exposure event occurred. Further burial occurred as the sediments of the Glenns Ferry Formation were deposited into the basin ~ 4 to 5 Ma. The combination of lithostatic pressure from the overburden of the Chalk Hills and Glenns Ferry sediments, sag, and down-dropping by a series of extensional faulting aided in the burial of the source rocks further until depths of thermal maturity were reached. In addition, basalt sill intrusions thought to be younger than 11 Ma (Wood, 2019), most likely increased the geothermal gradient in the basin as well, which aided maturation of the hydrocarbons.

The Willow field in the basin (Fig. 3) has proven to be the “sweet spot” where liquid condensate, natural gas, and oil all occur. In the Hamilton field to the south, the source may have become over mature, resulting in an area where oil does not occur. Not only maturation dictates the hydrocarbons that are possible in a field but also the kerogen type. Perhaps the Payette Formation is only one contributor to the hydrocarbons and other organic-rich rocks—possibly from the Mesozoic accreted terrane rocks at depth or to the north (Mann and Vallier, 2007)—are also contributors.

About 1400-2200 meters of sedimentary deposits are present above volcanic flows and sills in the subsurface (above volcanic units in logged sections in ML Investments 1-10 and Island Capital 1-9 in Fig. 10). Broad folds and normal faults expressed at the surface suggest these structures may form traps in the subsurface. Both 2D and 3D seismic surveys have been acquired and processed but are not available to the authors. More detailed fault and trap structure information is likely recorded by that data.

CONCLUSIONS

From the fossil evidence and geologic mapping, the Payette Formation is the sedimentary section interbedded within and deposited above the Miocene volcanic units north of the western Snake River Plain. The identification of *Liquidambar*, and its restriction to the Payette Formation, is critical. Some early definitions suggest that the formation only occurs as sedimentary interbeds between the larger volcanic units (CRBG and Weiser volcanics) of the Miocene. Here we suggest that the Payette should be defined as ~460 to 600 m of section above the last volcanic unit in addition to over ~460 m of sedimentary interbeds between the CRBG and Weiser volcanic intervals. The Poison Creek Formation is not mappable north of the WSRP and here we conclude that it either was not deposited, is indistinguishable from the Chalk Hills Formation, or it was eroded away before the Chalk Hills was deposited in that part of the basin. Here we suggest that the Poison Creek Formation be considered a member of the Chalk Hills Formation. The thickness of the Chalk Hills Formation is over 800 m in some wells.

The understanding of the Payette, Chalk Hills, and Glenns Ferry formations in surface exposures is important when attempting to correlate to the subsurface. These exposures provide an analogue for the play elements in the subsurface of Idaho's only producing field. For the first time, biostratigraphic markers have been defined for the oil and gas wells; this biostratigraphy was compared to new U/Pb ages of surface exposures to better understand fossil assemblages. These palynozones aid in the subsurface correlation from well to well and provide a stratigraphic framework and thickness of formations that has not yet been defined in the subsurface.

REFERENCES CITED

Allen, C.M., Campbell, I.H., 2012, Identification and elimination of a matrix-induced systematic error in LA–ICP–MS $^{206}Pb/^{238}U$ dating of zircon: Chemical Geology, v. 332-333, p. 157–165.

Armstrong, R.L., Leeman, W.P., and Malde, H.E., 1975, K-Ar dating, Quaternary and Neogene volcanic rocks of the Snake River Plain, Idaho: American Journal of Science, v. 275, p. 225-251.

Armstrong, R.L., Taubeneck, W.H., and Hales, P.O., 1977, Rb-Sr and K-Ar geochronometry of Mesozoic granitic rocks and their Sr isotopic composition, Oregon, Washington, and Idaho: Geological Society of America Bulletin, v. 88, p. 397-411.

Baghai, N.L., and Jorstad, R.B., 1995, Paleontology, paleoclimatology and paleoecology of the late Middle Miocene Musselshell Creek flora, Clearwater County Idaho. A preliminary study of a new fossil flora: Palaios, v. 10, no. 5, p. 424-436.

Barry, T.L., Kelley, S.P., Reidel, S.P., Camp, V.E., Self, S., Jarboe, N.A., Duncan, R.A., and Renne, P.R., 2013, Eruption chronology of the Columbia River Basalt Group, in Reidel, S.P., Camp, V.E., Ross, M.E., Wolff, J.A., Martin, B.S., Tolan, T.L., and Wells, R.E., eds., The Columbia River Flood Basalt Province: Geological Society of America Special Paper 497, p. 45-66.

Barton, M.D., 2019, Idaho Geological Survey Oil and Gas Program: GeoNote 46, online report: Idaho Geological Survey, accessed February 24th, 2020, https://www.idahogeology.org/product/g-46.

Benford, B., Crowley, J., Schmitz, M., Northrup, C.J., and Tikoff, B., 2010, Mesozoic magmatism and deformation in the northern Owyhee Mountains, Idaho: Implications for along-zone variations for the western Idaho shear zone: Lithosphere, v. 2, p. 93–118.

Benson, T.R., Mahood, G.A., and Grove, M., 2017, Geology and $^{40}Ar/^{39}Ar$ geochronology of the middle Miocene McDermitt volcanic field Oregon and Nevada; silicic volcanism associated with propagating flood basalt dikes at initiation of the Yellowstone hotspot: Geological Society of America Bulletin, v. 129, no. 9-10, p. 1027-1051.

Bestland, E.A., Forbes, M.S., Krull, E.S., Retallack, G.J. and Fremd, T, 2008. Stratigraphy, paleopedology, and geochemistry of the middle Miocene Mascall Formation (type area, central Oregon, USA): PaleoBios, v. 28, no. 2, p. 41-61.

Bingham, J.W., and Grolier, M.J., 1966. The Yakima basalt and Ellensburg formation of south-central Washington: Contributions to Stratigraphy: Geological Survey Bulletin 1124-G, p. G1-G15.

Bond, J. G, Kauffman, J. D., Rember, W. C., and Shiveler, D.J., 2011, Weiser basin evaluation: Idaho Geological Survey Technical Report T-11-1, p. 1-125.

Bonnichsen, B. and Kauffman, D.F., 1987, Physical features of rhyolite lava flows in the Snake River Plain volcanic province, southwestern Idaho: Geological Society of America Special Paper 212, p. 119-145.

Bonnichsen, B., Boroughs, S., Godchaux, M.M, and Wolff, J., 2016, From land to lake: Basalt and rhyolite volcanism in the Western Snake River Plain, Idaho, in Lewis, R.S., and Schmidt, K.L., eds., Exploring the Geology of the Inland Northwest: Geological Society of America Field Guide 41, p. 93-125.

Bowen, C.F., 1913, Contributions to economic geology from 1911: Part II, Mineral fuels--Coal at Horseshoe Bend and Jerusalem Valley, Boise County, Idaho, no. 531-H, p. 1-9.

Breedlovestrout R. L., and R. S. Lewis, 2017, Connecting geologic mapping to subsurface well logs to explore Idaho's first producing hydrocarbon field in Payette County: Geological Society of America Abstracts with Program, v, 49, no. 6.

Breedlovestrout R. L., Lewis R.S., Isakson V., Wood S., and Feeney, D.M., 2017, Mapping of Miocene-Pliocene Lake Idaho and Payette sedimentary deposits north of the western Snake River Plain: Geological Society of America Abstracts with Program, v. 49, no .6.

Buechler, W.K., Dunn, M.T., and Rember, W.C., 2007, Late Miocene Pickett Creek flora of Owyhee County, Idaho, in Contributions from the Museum of Paleontology: The University of Michigan, v. 31, no. 12, p. 305-362.

Buwalda, J.P., 1923, A preliminary reconnaissance of the gas and oil possibilities of southeastern and south-central Idaho: Idaho Bureau of Mines and Geology Pamphlet 5, 11 p.

Buwalda, J.P., 1924, The age of the Payette Formation and the old erosion surface in Idaho. Science, v. 60, no. 1564, p. 572-573.

Cahoon, E.B., Streck, M.J., Koppers, A.A.P., and Miggins, D.P., 2020, Reshuffling the Columbia River Basalt chronology- Picture Gorge Basalt, earliest- and longest- erupting formation: Geology, v. 48, https://doi.org/10.1130/G47122.1

Camp, V.E., and Ross, M.E., 2004, Mantle dynamics and genesis of mafic magmatism in the intermontane Pacific Northwest: Journal of Geophysical Research v. 109, no. B08204, 14 p.

Camp, V.E., Ross, M.E., Duncan, R.A., Jarboe, N.A., Coe, R.S., Hanan, B.B., and Johnson, J.A., 2013, The Steens Basalt: Earliest lavas of the Columbia River basalt Group, in Reidel, S.P., Camp, V.E., Ross, M.E., Wolff, J.A., Martin, B.S., Tolan, T.L., and Wells, R.E., eds., The Columbia River Basalt Province: Geological Society of America Special Paper 497, p. 87-116.

Capps, S.R., 1941, Faulting in western Idaho and its relation to the higher placer deposits: Idaho Bureau of Mines and Geology Pamphlet v. 56, 23 p.

Chaney, R.W., and D.I. Axelrod, 1959, Miocene floras of the Columbia Plateau: Carnegie Institution of Washington Publication 617, 237 p.

Condon, D.J., Schoene, B., McLean, N.M., Bowring, S.A., Parrish, R.R., 2015, Metrology and traceability of U-Pb isotope dilution geochronology (EARTHTIME Tracer Calibration Part I): Geochimica et Cosmochimica Acta, v. 164, p. 464–480.

Cope, E.D., 1883, A new Pliocene formation in the Snake River valley: American Naturalist, v. 17, p. 867-868.

Cummings, M.L., Evans, J.G., Ferns, M.L. and Lees, K.R., 2000, Stratigraphic and structural evolution of the middle Miocene synvolcanic Oregon-Idaho graben: Geological Society of America Bulletin, v. 112, no. 5, p. 668-682.

Dillhoff, R.M., Dillhoff, T.A., Dunn, R.E., Myers, J.A. and Strömberg, C.A., 2009, Cenozoic paleobotany of the John Day Basin, central Oregon: Volcanoes to Vineyards: geologic field trips through the dynamic landscape of the Pacific Northwest: Geological Society of America Field Guide, v. 15, p. 135-164.

Downing, K.F., and Swisher, C.C., III, 1993, New $^{40}Ar/^{39}Ar$ dates and refined geochronology of the Sucker Creek Formation, Oregon: Journal of Vertebrate Paleontology, v. 13, p. 33A.

Feeney, D.M., Garwood, D.L., Phillips, W.M, and Cooley, S.W., 2014, Geologic map of the Mann Creek SE quadrangle, Washington County, Idaho: Idaho Geological Survey Digital Web Map 169, scale 1:24,000, 1 sheet.

Feeney, D.M., and Phillips, W.M., 2016, Geologic map of the Midvale quadrangle, Washington County, Idaho: Idaho Geological Survey Digital Web Map 179, scale 1:24,000, 1 sheet.

Feeney, D.M., and Phillips, W.M., 2018, Geologic map of the Midvale Hill quadrangle, Washington County, Idaho: Idaho Geological Survey Digital Web Map 184, scale 1:24,000, 1 sheet.

Feeney, D.M., and Schmidt K.L., 2019, Geologic map of Crane Creek Reservoir quadrangle, Washington County, Idaho: Idaho Geological Survey Digital Web Map 187, scale 1:24,000, 1 sheet.

Feeney, D.M., Lewis, R.S., Phillips, W.M., Garwood, D.L., and Cooley, S.W., 2016a, Geologic Map of the Hog Creek Butte quadrangle, Washington and Adams counties, Idaho: Idaho Geological Survey Digital Web Map 174, scale 1:24,000, 1 sheet.

Feeney, D.M, Lewis, R.S., Isakson, V.H., Schmitz M.D., and Mertzman, S.A., 2016b, Refined stratigraphy of the Weiser embayment, west central, Idaho: Geological Society of America - Abstracts with Programs, v. 48, no. 6, 1 sheet.

Feeney, D.M., Isakson, V.H., Lewis, R.S., and Mertzman, S.A., 2017, Mapping middle Miocene volcanic rocks in the Weiser embayment, southwest Idaho: New U-Pb TIMS zircon age data and its implications: Geological Society of America Abstracts with Programs, v. 49, no. 6, doi: 10.1130/abs/2017AM-307041.

Feeney, D.M., Wood, S.H., Lewis, R.S., Phillips, W.M., Cooley S.W., and Garwood D.L., 2018, Geologic map of the Northeast Emmett quadrangle, Gem County, Idaho: Idaho Geological Survey Digital Web Map 185, scale 1:24,000, 1 sheet.

Fields, P. F., 1983, A review of the Miocene stratigraphy of southwestern Idaho, with emphasis on the Payette Formation and associated floras: University of California (Berkeley), M.A. Thesis, 386 p.

Fields, P. F., 1996, The Succor Creek Flora of the middle Miocene Sucker Creek Formation, southwestern Idaho and eastern Oregon: systematics and paleoecology: Michigan State University Ph. D. Dissertation, 700 p.

Fitzgerald, J.F., 1982, Geology and basalt stratigraphy of the Weiser embayment west-central, Idaho, in Bill Bonnichsen and R.M. Breckenridge, eds., Cenozoic Geology of Idaho: Idaho Bureau of Mines and Geology Bulletin v. 26, p. 103-128.

Forester, C.S., and Wood, S. H., 2012, Geologic map of the Holland Gulch quadrangle, Payette and Washington counties, Idaho: Idaho Geological Survey Technical Report 12-1, scale 1:24,000, 1 sheet.

Garwood, D.L., Feeney, D.M., Phillips, W.M., and Cooley, S.W., 2014, Geologic map of the Nutmeg Flat quadrangle, Washington County, Idaho: Idaho Geological Survey Digital Web Map 168, scale 1:24,000, 1 sheet.

Gilbert, J.D., Piety, L., and LaForge, R., 1983, Seismotectonic study Black Canyon Diversion Dam and Reservoir Boise Project, Idaho: U.S. Bureau of Reclamation Seismotectonic Report 83-7, 73 p.

Hart, W. K., and Brueseke, M.E., 1999, Analysis and dating of volcanic horizons from Hagerman Fossil Beds National Monument and a revised interpretation of eastern Glenns Ferry Formation chronostratigraphy: unpublished National Park Service Report 1443-PX9608-97-003, 37 p.

Hearst, J.M., 1999, The mammalian paleontology and depositional environments of the Birch Creek local fauna (Pliocene: Blancan), Owyhee County, Idaho. Papers on the vertebrate paleontology of Idaho honoring John A. White, v. 1, Idaho Museum of Natural History, p. 56-93.

Hooper, P.R., Camp, V.E., Reidel, S.P., Ross, M.E., 2007, The origin of the Columbia River flood basalt province: Plume versus nonplume models, in Foulger, G.R., and Jurdy, D.M., eds., Plates, plumes, and planetary processes: Geological Society of America Special Paper 430, p. 635-668.

Izett, G.A., 1981, Volcanic ash beds: Recorders of upper Cenozoic silicic pyroclastic volcanism in the western United States: Journal of Geophysical Research, v. 86, p. 10,200-10,222.

Jaffey, H., Flynn, K.F., Glendenin, L.E., Bentley, W.C., and Essling, A.M., 1971, Precision measurement of half-lives and specific activities of ^{235}U and ^{238}U: Physical Review, v. 4, p. 1889–1906.

Jarboe, N.A., Coe, R.S., Renne, P.R., and Glen, J.M.G., 2010, Age of the Steens reversal and the Columbia River Basalt Group: Chemical Geology, v. 274, p. 158-168.

Jijina, A.P, Currano, E.D., and Constenius, K., 2019, The paleobotany and paleoecology of the Eocene Herren beds of north-central Oregon, USA: Palaios, v. 34, no. 9, p. 424–436.

Kimmel, P.G., 1979, Stratigraphy and paleoenvironments of the Miocene Chalk Hills Formation and Pliocene Glenns Ferry Formation in the western Snake River Plain, Idaho, Ph.D. Dissertation, University of Michigan, 331 p.

Kimmel, P.G., 1982, Stratigraphy, age, and tectonic setting of the Miocene-Pliocene lacustrine sediments of the western Snake River Plain, Oregon and Idaho, in Bonnichsen, B., and Breckenridge, R.M. eds.,Cenozoic Geology of Idaho: Idaho Bureau of Mines and Geology Bulletin 26, p. 559-578.

Kirkham, V.R., 1930, Old erosion surfaces in southwestern Idaho: The Journal of Geology, v. 38, no. 7, p. 652-663.

Kirkham, V.R.D., 1931, Revision of the Payette and Idaho formations: Journal of Geology, v. 39, no. 5, p. 193-239.

Kirkham, V.R., and Johnson, M.M., 1929. The Latah Formation in Idaho: The Journal of Geology, v. 37, no. 5, p. 483-504.

Kasbohm, J. and Schoene, B., 2018, Rapid eruption of the Columbia River flood basalt and correlation with the mid-Miocene climate optimum: Science Advances, v. 4, no. 9, DOI: 10.1126/sciadv.aat8223.

Knowlton, F.H., 1926, Flora of the Latah Formation of Spokane, Washington, and Coeur d'Alene, Idaho: U.S. Geological Survey Professional Paper 140-A (Part II), p. 17-23.

Knudsen, K.L., Wong, I., Sawyer, T.L., Bott, J., Silva, W., and Lettis, W.R., 1996, Late Quaternary faulting and seismotectonics of east-central Oregon and west-central Idaho: Geological Society of America Abstracts with Programs, v. 28, p. 82.

Kohn, M.J., Miselis, J.L., and Fremd, T.J., 2002, Oxygen isotope evidence for progressive uplift of the Cascade Range, Oregon: Earth and Planetary Science Letters, v. 204, no. 1, p. 151–165.

Lawrence, D.C., 1988, Geology and revised stratigraphic interpretation of the Miocene Sucker Creek Formation, Malheur County, Oregon: Boise State University M.S. Thesis, 67 p.

Leopold, E.B. and Denton, M.F., 1987, Comparative age of grassland and steppe east and west of the northern rocky mountain: Annals of the Missouri Botanical Garden, v. 74, p. 841-867.

Lewis, R.S., Phillips, W.M., Feeney, D.M., Schmidt, K.L., and Wood, S.H., 2016, Geologic map of the Montour quadrangle, Gem and Boise counties, Idaho: Idaho Geological Survey Digital Web Map 177, scale 1:24,000, 1 sheet.

Lewis, R.S., Love, R.L., Wood, S.H., Othberg, K.L., Stanford, L.R., and Barton M., 2021 (in press), Geologic map of the Sheep Ridge quadrangle, Payette County, Idaho: Idaho Geological Survey Digital Web Map, scale 1:24,000, 1 sheet.

Lindgren, W., 1898, The mining districts of the Idaho Basin and the Boise Ridge, Idaho: U.S. Geological Survey Annual Report 13, no. 3, p. 617-744 and plates p. 87-102.

Link, P.K., McDonald, H.G., Fanning, C.M., and Godfrey, A.E., 2002, Detrital zircon evidence for Pleistocene drainage reversal at Hagerman Fossil Beds National Monument, central Snake River Plain, Idaho, in Bonnichsen, Bill, White, C.M., and McCurry, Michael, eds., Tectonic and Magmatic Evolution of the Snake River Plain Volcanic Province: Idaho Geological Survey Bulletin 30, p. 105-119.

Love R. L., Lewis R. S., and Feeney, D. M., 2021 (in press), Geologic Map of the Hog Cove Butte 7.5' quadrangle, Gem and Payette Counties, Idaho: Idaho Geological Survey, Digital Web Map, scale 1:24,000, 1 sheet.

Ludwig, K.R., 2003, User’s Manual for Isoplot 3.00. Berkeley Geochronology Center: Berkeley, CA, 70 p.

Macdonald, F.A., Schmitz, M.D., Strauss, J.V., Halverson, G.P., Gibson, T.M., Eyster, A., Cox, G., Mamrol, P., and Crowley, J.L., 2018, Cryogenian of Yukon: Precambrian Research, v. 319, p. 114–143.

Mackin, J.H., and Cary, A.S., 1965, Origin of Cascade landscapes: Washington Division of Mines and Geology Information Circular 41, 35 p.

Mahood, G.A., and Benson, T.R., 2017, Using ^{40}Ar/^{39}/Ar ages of intercalated silicic tuffs to date flood basalts: Precise ages for Steens Basalt Member of the Columbia River Basalt Group: Earth and Planetary Science Letters, v. 459, p. 340-351.

Malde, H.E., 1972, Stratigraphy of the Glenns Ferry Formation from Hammett to Hagerman, Idaho: U.S. Geological Survey Bulletin 1331-D, 19 p.

Malde, H.E., and Powers, H.A. 1962, Upper Cenozoic stratigraphy of western Snake River Plain, Idaho: Geological Society of America Bulletin, v. 73, no. 10, p. 1197-1220.

Mann, G.A., and Vallier, T.L., 2007, Mesozoic telescoping of island arc terranes and geologic evolution of the Cuddy Mountains region, western Idaho, *in* Kuntz, M.A., and Snee, L.W., eds., Geological Studies of the Salmon River Suture Zone and Adjoining Areas, West-Central Idaho and Eastern Oregon: U.S. Geological Survey Professional Paper 1738, p. 163–180.

Mapel, W.J., and Hail Jr, J., 1959, Tertiary Geology of the Goose Creek district, Cassia County, Idaho, Box Elder County, Utah, and Elko County, Nevada: U.S. Geological Survey Bulletin 1055-H, p. 217-254.

Mattinson, J.M., 2005, Zircon U–Pb chemical abrasion ("CA-TIMS") method: combined annealing and multi-step partial dissolution analysis for improved precision and accuracy of zircon ages: Chemical Geology, v. 220, no. 1-2, p. 47-66.

McKay, D.I.A., Tyrrell, T., Wilson, P.A. and Foster, G.L., 2014, Estimating the impact of the cryptic degassing of large igneous provinces: A mid-Miocene case-study: Earth and Planetary Science Letters, v. 403, p. 254-262.

McLean, N.M., Condon, D.J., Schoene, B., Bowring, S.A., 2015, Evaluating uncertainties in the calibration of isotopic reference materials and multi-element isotopic tracers (EARTHTIME Tracer Calibration Part II): Geochimica et Cosmochimica Acta, v. 164, p. 481–501.

Mitchell, S.G., and Montgomery, D.R., 2006, Polygenetic topography of the Cascade Range, Washington State, USA: American Journal of Science, v. 306, p. 736– 768, doi:10.2475/09.2006.03.

Morgan, W.J., 1972, Deep mantle convection plume and plate motions: American Association of Petroleum Geologists Bulletin, v. 56, p. 203-312.

Mustoe, G.E. and Leopold, E.B., 2014, Paleobotanical evidence for the post-Miocene uplift of the Cascade Range: Canadian Journal of Earth Sciences, v. 51, no. 8, p. 809-824.

Nasdala, L., Lengauer, C.L., Hanchar, J.M., Kronz, A., Wirth, R., Blanc, P., Kennedy, A.K., Seydoux-Guillaume, A.M., 2002, Annealing radiation damage and the recovery of cathodoluminescence: Chemical Geology, v. 191, p. 121–140.

Nash, B.P., and Perkins, M.E., 2012, Neogene fallout tuffs from the Yellowstone hotspot in the Columbia Plateau region, Oregon, Washington and Idaho, USA: PloS ONE, v. 7, no. 10, p. 1-13.

Neville, C., Opdyke, N.D. Lindsay, E.H., and Johnson, N.M., 1979, Magnetic stratigraphy of Pliocene deposits on the Glenns Ferry Formation, Idaho, and its implications for North American mammalian biostratigraphy: American Journal of Science, v. 279, p. 503-526.

Othberg, K.L., 1994, Geology and geomorphology of the Boise Valley and adjoining areas, western Snake River Plain, Idaho: Idaho Geological Survey Bulletin 29, 54 p.

Pardee, J.T., Bryan, K. and Knowlton, F.H., 1925, Geology of the Latah formation in relation to the lavas of Columbia Plateau near Spokane, Washington; and Flora of the Latah formation of Spokane, Washington, and Coeur d'Alene, Idaho: U.S. Geological Survey Professional Paper 140-A (Part I), 110 p.

Perkins, M.E., Brown, F.H., Nash, W.P., McIntosh, William, and Williams, S.K., 1998, Sequence, age, and source of silicic fallout tuffs in middle to late Miocene basins of the northern Basin and Range province: Geological Society of America Bulletin, v. 110, no. 3, p. 344-360.

Pierce, K. L., and Morgan, L. A., 1992, The track of the Yellowstone hot spot: Volcanism, faulting, and uplift, in Link, P. K., Kuntz, M. A., and Platt, L. B., eds., Regional geology of eastern and western Wyoming: Geological Society of America Memoir 179, p. 1–53.

Reidel, S.P., Tolan, T.L., Hooper, P.R., Beeson, M.H., Fecht, K.R., Bentley, R.D. and Anderson, J.L., 1989, The Grande Ronde Basalt, Columbia River Basalt Group; Stratigraphic descriptions and correlations in Washington, Oregon, and Idaho, in Reidel, S.P., and Hooper, P.R., eds., Volcanism and Tectonism in the Columbia River Flood-basalt Province: Geological Society of America Special Paper 239, p. 21-53.

Reidel, S.P., Camp, V.E., Tolan, T.L., and Martin, B.S., 2013, The Columbia River flood basalt province: Stratigraphy, areal extent, volume and physical volcanology, in Reidel, S.P., Camp, V.E., Ross, M.E., Wolff, J.A., Martin, B.S., Tolan, T.L., and Wells, R.E., eds., The Columbia River Basalt Province: Geological Society of America Special Paper 497, p. 1-43.

Reiners, P.W., Ehlers, T.A., Garver, J.I., Mitchell, S.G., Montgomery, D.R., Vance, J.A., and Nicolescu, S., 2002, Late Miocene exhumation and uplift of Washington Cascade Range: Geology, v. 30, p. 676–770, doi:10.1130/0091-7613.

Repenning, C.A., Weasman, T.R., and Scott, G.R., 1995, The early Pleistocene (latest Blancan-earliest Irvingtonian) Froman Ferry fauna and history of the Glenns Ferry Formation, southwestern Idaho: U.S. Geological Survey Bulletin 2105, 86 p.

Rivera, T.A., White, C.M., Schmitz, M.D., and Jicha, B.R., 2021, Petrogenesis of Pleistocene basalts from the Western Snake River Plain, Idaho: Journal of Petrology, v. 62, no. 3, p. egaa108, doi: 10.1093/petrology/egaa108.

Sander, K.T., and Wood, S.W., 2004, The Poison Creek Formation: A coarse fan-delta facies in the Miocene Chalk Hills Formation of the western Snake River Plain: Geological Society of America Abstracts with Programs, v. 36, no. 4 p. 92.

Savage, C.N., 1961, Geology and mineral resources of Gem and Payette counties: Idaho Bureau of Mines and Geology County Report 4, 50 p., scale 1:125,000, 1 sheet.

Schmitz, M.D. and Schoene, B., 2007, Derivation of isotope ratios, errors, and error correlations for U-Pb geochronology using ^{205}Pb-^{235}U-(^{233}U)-spiked isotope dilution thermal ionization mass spectrometric data: Geochemistry, Geophysics, Geosystems, v. 8, no. 8, 20 p. doi:10.1029/2006GC001492.

Shah, S. M. I., 1966, Stratigraphy and Paleobotany of the Weiser area: University of Idaho M.S. Thesis, 191 p.

Shah, S. M. I., 1968, Stratigraphic paleontology of the Weiser area, Idaho: University of Idaho Ph.D. Dissertation, 189 p.

Shervais, J.W., Shroff, G., Vetter, S.K., Matthews, S., Hanan, B.B., and McGee, J.J, 2002, Origin and evolution of the western Snake River Plain: Implications from stratigraphy, faulting, and the geochemistry of basalts near Mountain Home, Idaho, in B. Bonnichsen, C.M. White, and M. McCurry, eds., Tectonic and Magmatic Evolution of the Snake River Plain Volcanic Province: Idaho Geological Survey Bulletin 30, p. 343-361.

Smiley, C.J., 1963, The Ellensburg flora of Washington: California Publications in Geological Sciences, v. 35, no. 3, p. 159-276.

Smiley, C.J., 1989, The Miocene Clarkia fossil area of northern Idaho: Idaho Geological Survey Bulletin 28, p. 35-48.

Smiley, C.J., and Rember, W.C., 1985, Composition of the Miocene Clarkia flora, in Smiley, C.J., Leviton, A.E., and Berson, M., eds., Late Cenozoic History of the Pacific Northwest: American Association for the Advancement of Science, p. 95–112.

Smiley, C.J., Gray, J. and Huggins, L.M., 1975a, Preservation of Miocene fossils in unoxidized lake deposits, Clarkia, Idaho; with a section on fossil Insecta by W.F. Barr and J.M. Gillespie: Journal of Paleontology, v. 49, p. 833-844.

Smiley, C.J., Shah, S.M.I., and Jones, R.W., 1975b, Guidebook for the later Tertiary stratigraphy and paleobotany of the Weiser area, Idaho: Idaho Bureau of Mines and Geology Information Circular 28, p. 1-12.

Smith, G.A., 1988a, Neogene synvolcanic and syntectonic sedimentation in central Washington: Geological Society of America Bulletin, v. 100, no. 9, p. 1479-1492.

Smith, G.A., 1988b, Sedimentology of proximal to distal volcaniclastics dispersed across an active foldbelt: Ellensburg Formation (late Miocene), central Washington: Sedimentology, v. 35, no. 6, p. 953-977.

Smith, R.B. and Braile, L.W., 1994, The Yellowstone hotspot: Journal of Volcanology and Geothermal Research, v. 61, no. 3-4, p. 121-187.

Smith, G, and Cossel, J., Jr., 2002, Fishes from the late Miocene Poison Creek and Chalk Hills formations, Owyhee County, Idaho, in Akersten, W.A., Thompson, M.E., Meldrum, D.J., Rapp, R.A., and McDonald, H.G., eds., Papers on the Vertebrate Paleontology of Idaho Honoring John A. White, v. 2: Idaho Museum of Natural History Occasional Paper 37, p. 23-35.

Smith, G.R., Swirydczuk, K., Kimmel, P.G. and Wilkinson, B.H., 1982, Fish biostratigraphy of late Miocene to Pleistocene sediments of the western Snake River Plain, Idaho, in Bonnichsen, B., and Breckenridge, R.M., Cenozoic Geology of Idaho: Idaho Bureau of Mines and Geology Bulletin, 26, p. 519-541.

Smith, G.A., Shafiqullah, M., Campbell, N.P. and Deacon, M.W., 1989, Geochronology of the Ellensburg Formation—Constraints on Neogene volcanism and stratigraphic relationships in central Washington: Isochron/West, v. 53, p. 28-32.

Smith, G.R., Morgan, N., and Gustafson, E., 2000, Fishes of the Mio-Pliocene Ringold Formation, Washington: Pliocene capture of the Snake River by the Columbia River: University of Michigan Papers on Paleontology, v. 32, p. 1–47.

Swanson, D.A., Wright, T.L., Hooper, P.R. and Bentley, R.D., 1979, Revisions in stratigraphic nomenclature of the Columbia River Basalt Group: U.S. Geological Survey Bulletin 1457-G, 59 p.

Swirydczuk, K., Wilkinson, B.H. and Smith, G.R., 1981, Synsedimentary lacustrine phosphorites from the Pliocene Glenns Ferry Formation of southwestern Idaho: Journal of Sedimentary Research, v. 51, no. 4, p. 1205-1214.

Swirydczuk, K., Wilkinson, B.H., and Smith, G.R., 1979, The Pliocene Glenns Ferry oolite; lake-margin carbonate deposition in the southwestern Snake River Plain: Journal of Sedimentary Research, v. 49, no. 3, p. 995-1004.

Swirydczuk, K., Wilkinson, B.H., and Smith, G.R., 1980, The Pliocene Glenns Ferry Oolite; II, Sedimentology of oolitic lacustrine terrace deposits: Journal of Sedimentary Research, v. 50, no. 4, p. 1237-1247.

Swirydczuk, K., Larson, G.P., and Smith, G.R., 1982, Volcanic ash beds as stratigraphic markers in the Glenns Ferry and Chalk Hills Formations from Adrian, Oregon, to Bruneau, Idaho, in Bonnichsen, B., and Breckenridge, R.M., eds., Cenozoic Geology of Idaho: Idaho Bureau of Mines and Geology Bulletin 26, p. 543-558.

Taggart, R.E., Cross, A.T., Dilcher, D.L. and Taylor, T.N., 1980, Vegetation change in the Miocene Sucker Creek flora of Oregon and Idaho: A case study in paleosuccession. biostratigraphy of fossil plants, in Dilcher, D. L., and Taylor, T. N., eds, Biostratigraphy of fossil plants: Stroudsburg: Dowden, Huchinson, and Ross, Inc., p. 185-221.

Viney, M., Mustoe, G.E., Dillhoff, T.A., and Link, P.K., 2017, The Bruneau Woodpile: A Miocene phosphatized fossil wood locality in southwestern Idaho, USA: Geosciences, v. 7, no. 3, 25 p.

Warner, M.M., 1975, Special aspects of Cenozoic history of southern Idaho and their geothermal implications: In Proc. 2nd United Nations Symposium on the Development and Use of Geothermal Resources, p. 653-664.

Wendt, I., and Carl, C., 1991, The statistical distribution of the mean squared weighted deviation: Chemical geology. Isotope geoscience section, v. 86, no. 4, p. 275–285.

Wheeler, H.E., and Cook, E.F., 1954, Structural and stratigraphic significance of the Snake River capture, Idaho-Oregon: Journal of Geology, v. 62, p. 525-536.

Wood, S.H., 1994, Seismic expression and geological significance of a lacustrine delta in Neogene deposits of the western Snake River plain, Idaho: American Association of Petroleum Geologists Bulletin, v. 78, no. 1, p. 102-121.

Wolfe, J.A., 1995, Paleoclimatic estimates from Tertiary leaf assemblages: Annual Review of Earth and Planetary Sciences, v. 23, no. 1, p. 119-142.

Wood, S. H., and Clemens, D. M., 2002, Geologic and tectonic history of the western Snake River Plain, Idaho and Oregon, in Bonnichsen, B., White, C.M., and McCurry, M., eds., Tectonic and Magmatic Evolution of the Snake River Plain Volcanic Province: Idaho Geological Survey Bulletin 30, p. 69-103.

Wood, S.H., 2019, Multiple basalt sill intrusions into the Miocene Payette/Drip Springs and lower Chalk Hills Formation sediments, 1.4-2.4 km deep beneath Ontario, Oregon: Identification and significance for Western Snake River Plain stratigraphy: Geological Society of America Abstracts with Programs.

Wood, S.H., 2004, Geology across and under the western Snake River Plain, Idaho: Owyhee Mountains to the Boise Foothills (Chapter 7), in Haller, K.M. and Wood, S.H. (eds.), Geological Field trips in Southern Idaho, Eastern Oregon, and Northern Nevada: U. S. Geological Survey Open-File Report 2004-1222, p. 84-107.

Zachos, J., Pagani, M., Sloan, L., Thomas, E. and Billups, K., 2001, Trends, rhythms, and aberrations in global climate 65 Ma to present: Science, v. 292, no. 5517, p. 686-693.

TABLE CAPTIONS

Table 1. CA-IDTIMS U-Pb isotopic data for zircons from silicic volcanic rocks collected near Emmett, Idaho.

Table 2. Scientific and common names for plant macro- and microfossils.

Table 3. Surface palynomorph samples and macrofossils. Note palynomorphs that are described for specific U/Pb dates.

Table 4. Identified palynomorphs in each of the Bridge and Paramax Resources subsurface wells. The presence of a palynomorph grain is indicated by a "1." Designations: PF = Payette Formation, CH = Chalk Hills Formation, GF = Glenns Ferry Formation

FIGURE CAPTIONS

Figure 1. Simplified geologic map of southwest Idaho and southeast Oregon showing the distribution of volcanic and sedimentary strata.

Figure 2. Regional stratigraphy and graphical composite stratigraphic section of the Glenns Ferry, Chalk Hills, and Payette formations north of the WSRP. Compilation from Wood (1994), Haq et al. (1987), Zachos et al. (2001), Wood and Clemens (2002), and Reidel et al. (2003).

Figure 3: Study area with mapped geology and sample locations for U/Pb ages and fossil localities. Grid lines in background refer to quadrangle boundaries. HG = Holland Gulch, PVR = Paddock Valley Reservoir, SR = Sheep Ridge, HCB = Hog Cove Butte, SB = Squaw Butte, NEE = Northeast Emmett, and MO = Montour quadrangles. Refer to Table 1 for age information and Table 3 for more detailed description of fossil locality. Note A-A’ (solid line) for cross section in Figure 4 and B-B’ (dashed line) for correlated well traverse in Figure 10.

Figure 4. Cross section A-A' from the Ore-Ida well east-northeast to the edge of the Idaho batholith. West-southwest part of section is based on well data; east-northeast part is based only on surface mapping and dip projection.

Figure 5: Left diagram shows index pollen grains plotted against subsurface well depth. Pollen shown were significant for formation designations. Photographs in the middle are A: Artemesia, B: Asteraceae, C: Cedrus, D: Chenopodiaceae, E: Ephedra, F: Liquidambar, G: Poaceae/Graminea, H: Platanus, I: Pterocarya. Right diagram is a seriation plot (presence vs.

absence diagram) that shows common index grains to the Glenns Ferry (GF), Chalk Hills (CH) and Payette (PF) formations.

Figure 6. Photographs of field outcrops, thin sections, and hand samples for the Payette Formation. A Indian Creek lignite in southeast Paddock Valley Reservoir quadrangle, B: Ash containing localized ostracodes in Alkali Creek, Paddock Valley Reservoir quadrangle, C: Ash and sand south of Crane Creek Reservoir, 10.5 km north of Paddock Valley Reservoir; D: Looking southeast at Alkali Creek in the Hog Cove Butte quadrangle, showing the general southwest downwarp of the sediments; E: Sandstone in the well cuttings of ML Investments at 6280' MD; F: Lapilli-rich, unwelded tuff south of Indian Creek in the Paddock Valley quadrangle, dated at 15.88 Ma; G: Fossil leaves in the densely welded tuff above photo; H: Ash bed northeast of Sulfur Gulch in the Hog Cove Butte quadrangle.

Figure 7. Photographs of field outcrops, thin sections, and hand samples for the Poison Creek Formation (A) and Chalk Hills Formation (B-I). A: Rhyolite and sand clasts in the Poison Creek Formation in Poison Creek, south of the WSRP, scale is in mm; B: Ash east of Emmett, (15RL014) dated at 9.04 Ma; C: Pumice-rich outcrop at the Haw Creek locality (15RL015a) dated at 9.01 Ma D: Tuffaceous mudstone underlying oxidized sand that represents the Glenns Ferry/Chalk Hills formation contact in the Bannister Basin, Hog Cove Butte quadrangle, E: Fish fossils in the upper Chalk Hills, Bannister Basin; F: Ash in the central Hog Cove Butte quadrangle with a chemical match to an ash east of Emmett dated at 9.04 Ma (15RL014); G: Pumice from Sulfur Gulch (16RLB014), Hog Cove Butte quadrangle, dated at 7.78 Ma, S. H.

Wood circled for scale H: Close up of the pumice in photo G; I: Uppermost Chalk Hills Formation, eastern Sheep Ridge quadrangle.

Figure 8. Photographs of field outcrops, thin sections, and hand samples for the Glenns Ferry Formation. A: Outcrop in southeast Birding Island quadrangle; B: Mudstone interval in southeast Hog Cove Butte quadrangle, C: Diatoms in the cuttings from Espino 1-2 well at 450' MD; D: Ooid bed in the southeast corner of the Hog Cove Butte quadrangle; E: Close up of the ooids in photo D with fish fossils; F: Fish fossils from outcrop in photo D; G: Ash bed southern Sheep Ridge quadrangle, H: Lithified oolite beds 12 km northeast of Weiser; and I: Sand with fish fossils in the northern Sheep Ridge quadrangle.

Figure 9: Plot of $^{206}Pb/^{238}U$ dates from grains of analyzed by ID-TIMS. Plotted with Isoplot 3.0 (Ludwig, 2003). Error bars are at 2 sigma. Weighted mean dates are shown and represented by gray boxes behind the error bars. White boxes represent dates not used in weighted mean calculations.. A: CL images of zircon grains from 15RL015A, B: 16RLB014 Sulfur Gulch, C: 15RL015a Haw Creek, D: 15RL014, E. of Emmett, E: 15DF415 Indian Creek, F: 16DF438 Indian Creek

Figure 10: Well top mapping based on stratigraphic packages and new palynology data. Wells also are depicted in the cross-section. Scales for logs (from left to right) are: Gamma Ray (GR) 0-260 gAPI; Density (DENS) 1.3-2.95 g/cm3; Neutron Porosity (NPHI) 0.0085-80. LOG = drafted from well cutting samples taken at 10-foot intervals. MD = measured depth.

Figure 11: Wheeler Diagram showing chronostratigraphic relationship and major hiatuses. Note: Payette Formation is of limited lateral extent near Weiser and Horseshoe Bend. The Chalk Hills and Glenns Ferry formations are much more laterally extensive (full extent not shown here). Poison Creek Formation is not depicted because it does not occur in diagram area.

Table 1. CA-IDTIMS U-Pb isotopic data for zircons from silicic volcanic rocks collected near Emmett, Idaho

	Compositional Parameters						Radiogenic Isotope Ratios									Radiogenic Isotope Dates					
Sample (a)	Th/U (b)	$^{206}Pb^*$ x10^{-13} mol (c)	mol % $^{206}Pb^*$ (c)	Pb^*/Pb_c (c)	Pb_c (pg) (c)	$^{206}Pb/^{204}Pb$ (d)	$^{208}Pb/^{206}Pb$ (e)	$^{207}Pb/^{206}Pb$ (e)	% err (f)	$^{207}Pb/^{235}U$ (e)	% err (f)	$^{206}Pb/^{238}U$ (e)	% err (f)	corr. coef.	$^{207}Pb/^{206}Pb$ (g)	± (f)	$^{207}Pb/^{235}U$ (g)	± (f)	$^{206}Pb/^{238}U$ (g)	± (f)
16RLB014, Sulfer Gulch, Chalk Hills Fm, rhyolitic pumice, N44.0690°, W116.5350°																				
z7	0.529	0.0170	80.96%	1.3	0.33	95	0.172	0.048944	13.2	0.008168	13.45	0.0012104	0.586	0.378	145	309	8.26	1.11	**7.798**	**0.046**
z10	0.548	0.0522	86.93%	2.0	0.65	138	0.178	0.046791	3.6	0.007797	3.81	0.0012086	0.345	0.748	39	85	7.89	0.30	**7.786**	**0.027**
z8	0.559	0.0312	88.41%	2.3	0.34	156	0.182	0.047568	4.6	0.007924	4.76	0.0012082	0.323	0.586	78	108	8.01	0.38	**7.784**	**0.025**
z1	0.473	0.0718	89.76%	2.6	0.68	176	0.154	0.044865	2.8	0.007463	3.04	0.0012065	0.271	0.749	-63	69	7.55	0.23	**7.773**	**0.021**
z4	0.524	0.0369	83.38%	1.5	0.61	109	0.170	0.045337	7.8	0.007540	8.08	0.0012062	0.467	0.518	-38	189	7.63	0.61	**7.771**	**0.036**
z6	0.526	0.0205	80.40%	1.2	0.41	92	0.171	0.046143	10.6	0.007673	10.87	0.0012061	0.586	0.509	5	254	7.76	0.84	**7.770**	**0.045**
z9	0.515	0.0197	85.47%	1.8	0.28	124	0.167	0.046982	10.7	0.007806	10.87	0.0012051	0.423	0.363	48	255	7.90	0.85	**7.764**	**0.033**
z3	0.460	0.0173	79.80%	1.2	0.36	89	0.149	0.044693	13.6	0.007413	13.80	0.0012030	0.585	0.404	-72	330	7.50	1.03	**7.750**	**0.045**
										weighted mean $^{206}Pb/^{238}U$ age = 7.776 ± 0.013 (0.013) [0.016] Ma (95% c.i.); MSWD = 0.54 (n=8) (h)										
15RL015a, Haw Creek, Chalk Hills Fm, rhyolitic pumice, N43.9642°, W116.4879°																				
z2	0.588	0.0049	67.42%	1	0.20	55	0.191	0.046232	181.0	0.008968	181.04	0.0014069	0.861	0.084	10	4335	9.07	16.34	9.063	0.078
z6	0.860	0.0155	87.24%	2	0.19	141	0.278	0.045986	14.7	0.008877	14.76	0.0014000	0.302	0.329	-3	352	8.97	1.32	**9.018**	**0.027**
z3	0.903	0.0159	86.83%	2	0.20	137	0.292	0.045706	7.5	0.008822	7.65	0.0013999	0.257	0.534	-18	181	8.92	0.68	**9.018**	**0.023**
z1	0.870	0.0178	87.23%	2	0.22	141	0.282	0.046561	7.9	0.008982	7.98	0.0013991	0.256	0.494	27	188	9.08	0.72	**9.013**	**0.023**
z5	0.847	0.0106	82.10%	2	0.19	101	0.274	0.046785	28.6	0.009018	28.65	0.0013980	0.392	0.216	38	681	9.12	2.60	**9.006**	**0.035**
z7	0.917	0.0621	94.81%	6	0.28	348	0.297	0.044698	1.6	0.008611	1.71	0.0013972	0.133	0.823	-72	39	8.71	0.15	**9.001**	**0.012**
z4	0.933	0.0159	86.85%	2	0.20	137	0.302	0.044335	10.4	0.008531	10.53	0.0013956	0.258	0.384	-92	255	8.63	0.90	**8.991**	**0.023**
										weighted mean $^{206}Pb/^{238}U$ age = 9.005 ± 0.015 (0.016) [0.018] Ma (95% c.i.); MSWD = 0.43 (n=6) (h)										
15RL014, East of Emmett, Chalk Hills Fm, felsic lapilli tuff, N43.8866°, W116.4343°																				
z3	0.685	0.0764	77.05%	1	1.89	79	0.222	0.047477	6.8	0.009213	7.24	0.0014074	0.672	0.744	73	160	9.31	0.67	**9.066**	**0.061**
z7	0.655	0.0384	90.06%	3	0.35	182	0.212	0.045403	3.4	0.008800	3.55	0.0014058	0.293	0.665	-34	81	8.90	0.31	**9.056**	**0.027**
z1	0.861	0.0546	83.50%	2	0.89	109	0.279	0.043893	5.1	0.008503	5.48	0.0014050	0.474	0.734	-117	126	8.60	0.47	**9.051**	**0.043**
z8	0.646	0.0259	84.44%	2	0.40	116	0.209	0.046993	6.5	0.009099	6.76	0.0014042	0.441	0.571	49	155	9.20	0.62	**9.046**	**0.040**
z6	0.505	0.0190	84.16%	2	0.30	114	0.164	0.043416	8.4	0.008404	8.65	0.0014039	0.480	0.533	-144	207	8.50	0.73	**9.044**	**0.043**
z4	0.561	0.0553	86.24%	2	0.73	131	0.182	0.045528	4.1	0.008808	4.33	0.0014031	0.379	0.745	-27	98	8.90	0.38	**9.039**	**0.034**
z5	0.778	0.0228	83.78%	2	0.37	111	0.252	0.045608	10.4	0.008800	10.56	0.0013994	0.470	0.434	-23	250	8.90	0.94	**9.015**	**0.042**
z2	0.559	0.0437	84.90%	2	0.65	120	0.181	0.043828	6.0	0.008453	6.30	0.0013987	0.449	0.668	-120	148	8.55	0.54	**9.010**	**0.040**
										weighted mean $^{206}Pb/^{238}U$ age = 9.041 ± 0.016 (0.016) [0.019] Ma (95% c.i.); MSWD = 0.86 (n=8) (h)										
14RL065, SW of Montour, Chalk Hills Fm, felic lapilli tuff, N43.8837°, W116.3708°																				
z8	0.388	4.2298	99.79%	140	0.74	8689	0.123	0.059704	0.1	0.363606	0.13	0.0441696	0.065	0.959	593	2	314.9	0.36	278.6	0.177
z7	0.531	0.7542	99.00%	30	0.63	1825	0.171	0.046447	0.2	0.015178	0.28	0.0023701	0.076	0.670	21	6	15.30	0.04	15.261	0.012
z2	0.719	0.2155	95.92%	8	0.76	447	0.232	0.048891	0.8	0.012024	0.85	0.0017837	0.114	0.680	143	18	12.14	0.10	11.488	0.013
z5	0.448	0.0235	67.83%	1	0.92	57	0.145	0.044907	21.0	0.010400	21.17	0.0016796	0.683	0.280	-61	510	10.51	2.21	10.819	0.074
z3	0.703	0.0862	92.96%	4	0.54	257	0.228	0.046907	1.7	0.010659	1.78	0.0016481	0.177	0.755	45	39	10.77	0.19	10.616	0.019
z4	0.476	0.0736	91.35%	3	0.58	210	0.154	0.046764	2.4	0.010468	2.50	0.0016234	0.200	0.714	37	56	10.57	0.26	10.457	0.021
z13	0.752	0.0080	61.29%	1	0.42	47	0.243	0.049744	28.7	0.011025	29.25	0.0016074	1.394	0.402	183	667	11.13	3.24	10.354	0.144
z9a	0.861	0.0315	88.94%	3	0.32	163	0.279	0.045878	4.0	0.010090	4.19	0.0015950	0.302	0.632	-9	96	10.19	0.42	10.274	0.031
z9b	0.814	0.0223	69.88%	1	0.79	61	0.263	0.047282	8.6	0.010336	8.96	0.0015855	0.651	0.634	64	203	10.44	0.93	10.213	0.066
z12	0.708	0.0151	69.75%	1	0.54	60	0.229	0.037769	23.0	0.008219	23.44	0.0015783	0.931	0.446	-501	611	8.31	1.94	10.167	0.095
z11	0.386	0.0803	92.58%	4	0.53	244	0.125	0.044924	3.1	0.009575	3.21	0.0015458	0.196	0.646	-60	75	9.68	0.31	9.957	0.020
z6	0.416	0.0664	90.33%	3	0.59	187	0.135	0.046541	2.4	0.009858	2.53	0.0015362	0.223	0.734	26	57	9.96	0.25	**9.896**	**0.022**

Table 1. CA-IDTIMS U-Pb isotopic data for zircons from silicic volcanic rocks collected near Emmett, Idaho

	Compositional Parameters						Radiogenic Isotope Ratios								Radiogenic Isotope Dates					
Sample (a)	$\frac{Th}{U}$ (b)	$^{206}Pb^*$ $\times 10^{-13}$ mol (c)	mol % $^{206}Pb^*$ (c)	$\frac{Pb^*}{Pb_c}$ (c)	Pb_c (pg) (c)	$\frac{^{206}Pb}{^{204}Pb}$ (d)	$\frac{^{208}Pb}{^{206}Pb}$ (e)	$\frac{^{207}Pb}{^{206}Pb}$ (e)	% err (f)	$\frac{^{207}Pb}{^{235}U}$ (e)	% err (f)	$\frac{^{206}Pb}{^{238}U}$ (e)	% err (f)	corr. coef.	$\frac{^{207}Pb}{^{206}Pb}$ (g)	± (f)	$\frac{^{207}Pb}{^{235}U}$ (g)	± (f)	$\frac{^{206}Pb}{^{238}U}$ (g)	± (f)
15DF415, Indian Creek, Payette Fm, dacitic lapilli tuff, N44.1731°, W116.5899°																				
z3	0.593	0.0582	92.28%	4	0.40	234	0.191	0.045420	2.7	0.015555	2.88	0.0024839	0.233	0.723	-33	66	15.67	0.45	15.992	0.037
z7	0.564	0.0617	92.39%	4	0.42	237	0.182	0.046428	2.0	0.015873	2.11	0.0024797	0.201	0.748	20	47	15.99	0.33	15.965	0.032
z6	1.769	0.3909	99.13%	46	0.28	2072	0.569	0.046347	0.3	0.015832	0.35	0.0024774	0.114	0.513	16	8	15.95	0.06	15.951	0.018
z5	0.503	0.0966	92.87%	4	0.62	253	0.162	0.046933	1.8	0.015983	1.94	0.0024700	0.188	0.754	46	43	16.10	0.31	**15.903**	**0.030**
z4	0.484	0.0672	90.86%	3	0.56	197	0.156	0.046059	3.2	0.015675	3.40	0.0024683	0.275	0.669	1	78	15.79	0.53	**15.892**	**0.044**
z2	0.543	0.1346	95.10%	6	0.58	368	0.175	0.046160	1.5	0.015709	1.57	0.0024682	0.146	0.727	6	35	15.83	0.25	**15.891**	**0.023**
z1	0.654	0.2031	96.23%	8	0.66	478	0.211	0.046082	1.1	0.015658	1.18	0.0024643	0.112	0.820	2	26	15.78	0.18	**15.866**	**0.018**
										weighted mean $^{206}Pb/^{238}U$ age = 15.882 ± 0.020 (0.021) [0.027] Ma (95% c.i.); MSWD = 1.84 (n=4) (h)										
16DF438, Indian Creek, rhyolite of Indian Creek, N44.1403°, W116.5865°																				
z11	0.483	0.0561	95.62%	6.5	0.21	412	0.156	0.046331	1.9	0.016282	1.97	0.0025488	0.163	0.742	15	44	16.40	0.32	**16.410**	**0.027**
z3	0.460	0.0507	89.58%	2.6	0.49	173	0.148	0.045726	3.0	0.016062	3.20	0.0025477	0.269	0.766	-17	72	16.18	0.51	**16.402**	**0.044**
z5	0.477	0.1872	96.98%	9.6	0.48	597	0.154	0.045881	0.9	0.016108	0.96	0.0025463	0.117	0.631	-9	22	16.23	0.15	**16.393**	**0.019**
z6	0.423	0.0501	93.46%	4.2	0.29	276	0.136	0.044520	2.5	0.015630	2.62	0.0025463	0.190	0.671	-82	61	15.75	0.41	**16.393**	**0.031**
z10	0.432	0.0958	95.55%	6.3	0.37	406	0.139	0.046175	1.3	0.016210	1.36	0.0025461	0.141	0.698	7	30	16.33	0.22	**16.393**	**0.023**
z7	0.424	0.0675	96.05%	7.2	0.23	457	0.137	0.046995	1.4	0.016497	1.46	0.0025459	0.132	0.716	49	33	16.61	0.24	**16.391**	**0.022**
z8	0.731	0.1124	97.53%	13	0.24	730	0.236	0.046858	0.7	0.016436	0.81	0.0025439	0.112	0.630	42	18	16.55	0.13	**16.378**	**0.018**
										weighted mean $^{206}Pb/^{238}U$ age = 16.395 ± 0.009 (0.011) [0.021] Ma (95% c.i.); MSWD = 0.72 (n=9) (h)										

(a) z1, z2 etc. are labels for single zircon grains or fragments annealed and chemically abraded after Mattinson (2005); **bold** indicates results used in weighted mean calculations.
(b) Model Th/U ratio iteratively calculated from the radiogenic 208Pb/206Pb ratio and 206Pb/238U age.
(c) Pb* and Pbc represent radiogenic and common Pb, respectively; mol % $^{206}Pb^*$ with respect to radiogenic, blank and initial common Pb.
(d) Measured ratio corrected for spike and fractionation only. Pb isotope fractionation estimated from ET2535 (202Pb-205Pb) spiked samples run during the same analytical period; U fractionation calculated from the measured ET535 (233U-235U) spike ratio.
(e) Corrected for fractionation, spike, and common Pb; all common Pb was assumed to be procedural blank: 206Pb/204Pb = 18.042 ± 0.61%; 207Pb/204Pb = 15.537 ± 0.52%; 208Pb/204Pb = 37.686 ± 0.63% (all uncertainties 1-sigma).
(f) Errors are 2-sigma, propagated using the algorithms of Schmitz and Schoene (2007).
(g) Calculations are based on the decay constants of Jaffey et al. (1971). 206Pb/238U and 207Pb/206Pb ages corrected for initial disequilibrium in 230Th/238U using Th/U [magma] = 3.
(h) Age uncertainties reported at the 95% confidence interval, as ± analytical (+tracer) [+decay constant]; MSWD = mean squared weighted deviation. *The 95% confidence interval is the internal standard deviation multiplied by the Student's t-distribution multiplier for a two-tailed 95% critical interval and n-1 degrees of freedom for MSWD < 1+2*sqrt[2/(n-1)] (Wendt and Carl, 1991), and expanded via multiplication by the sqrt(MSWD) when the MSWD ≥ 1+2*sqrt[2/(n-1)], in order to accommodate unknown sources of overdispersion.

Table 2

Scientific Name	Common Name
Abies	Fir
Acer	Maple
Alnus	Alder
Amaranthaceae	Amaranths
Artemesia	Mugwort, wormwood, sagebrush
Asteraceae/Compositae	Aster, daisy, composite, sunflower family
Berberis	Barberry
Betula	Birch
Carpinus	Hornbeam
Carya	Hickory
Caryophyllaceae	Carnation
Castenea	Chestnut
Cathaya	Pine family
Cedrela	Melaceae family
Cedrus	Cedar
Celtis	Hackberry, Nettle tree
Cercidophyllum	Katsura
Chamaecyparis	False Cypress
Chenopodiaceae	Saltbrush
Cornus	Dogwood
Eleagnus	Silverberry
Ephedra	Mormon Tea
Equisetum	Horsetail, Scouring Rush
Ericaceae	Heather
Fabaceae	Legume, pea, bean family
Fagaceae	Beech family
Fagus	Beech
Fraxinus	Olive and Lilac
Ginkgo	Ginkgo
Glyptostrobus	Chinese Water Pine
Humulus	Hop
Ilex	Holly
Isoetes	Quillwort

Scientific Name	Common Name
Larix	Larch
Lauraceae	Laurels
Liquidambar	Sweetgum
Lithocarpus	Stone Oak
Metasequoia	Dawn Redwood
Myrica	Bayberry, wax-myrtle
Myriophyllum	Water Milfoil family
Nymphaea	Water Lily
Nyssa	Tupelo
Onagraceae	Evening Primose family
Opuntiodeae	Cactus
Ostrya	Hop-Hornbeam
Picea	Spruce
Pinus	Pine
Platanus	Sycamore
Poaceae/Graminae	Grasses
Podocarpus	Podocarp family (yellowwood)
Pseudotsuga	Douglas Fir
Pterocarya	Wingnut
Quercus	Oak
Rhus	Sumac
Rosaceae	Roses and other edible fruit trees
Salix	Willow
Sarcobatus	Greasewood
Sassafras	Sassafras
Saxifragaceae	Saxifrage family
Sequoia	Redwood
Tamarix	Athel tree
Taxodium/Cuppressaceae	Cypress
Taxus	Yew
Tilia	Basswood/Linden
Tsuga	Hemlock
Ulmus/Zelkova	Elm

Juglans	Walnut
Juniperus	Juniper
Veronica	Gypsyweed

Table 3

Mapped Fm	Sample	Lithology	Quadrangle, Location	Latitude, Longitude	U/Pb date (Ma)	Extraction	Microfossils	Macrofossils
Chalk Hills	xx1: 15RLB017	tuffaceous fine sandstone	NE Emmett, Haw Creek Roadcut	43.9642, -116.488	9.0057 ± 0.0082(ID-TIMS) near fossil site (sample 15RL014)	Poor	Taxodiaceae/Cuppressaceae/Taxodium, *Pseudotsuga/Larix*	*Quercus, Juglans, Metasequoia*
	xx2: 15RLB022	fine greywacke	NE Emmett, train tunnel			Poor	*Pterocarya, Alnus,* Chenopodiaceae, *Ulmus?,* Caryophyllaceae, Taxodiaceae/Cuppressaceae/Taxodium, Monolete spore	
	xx3: 16RLB019	tan silt-claystone below ash #3 at pumice site	Hog Cove Butte, Sulfur Gulch, Pumice #1	44.069, -116.535	7.779 ± 0.010 (ID-TIMS)	Good	*Pterocarya,* Taxodium/Cuppressaceae, *Picea, Juglans, Abies, Betula, Pinus, Alnus, Ostrya, Tilia?,* Chenopodiaceae cf. *austria*	
	xx4: 16RLB026 A	d. grey silt-claystone below pumice	Hog Cove Butte, Bannister Basin, Pumice #2	44.069, -116.535	7.779 ± 0.010 (ID-TIMS)	Good	*Pinus, Alnus, Castenea, Taxus,* Taxodium/Cuppressaceae, *Picea, Quercus, Abies, Carya, Platanus, Nyssa?, Juglans?, Tsuga, Pterocarya, Podocarpus* or *Cathaya*, Chenopodiaceae cf. *Sarcobatus*, Chenopodiaceae, *Acer*? Eriacaceae?, Pseudotsuga/Larix	
	xx5: 17RL252	brown-grey fine sandstone	NE Emmett, fossil site	43.9715, -116.4870		Fair	*Pterocarya, Alnus*, Taxodium/Cuppressaceae, Chenopodiaceae	

Payette	xx6: 15RLB010	muddy lignite	Paddock Valley, Indian Creek FL6	44.1417, -116.5827	16.394 ± 0.008 (ID-TiMS)	Moderate	*Juglans, Rhus, Nymphaea, Liquidamber, Betula, Alnus, Taxus, Ulmus, Picea,* Taxodiaceae/Cuppressaceae/Taxodium, *Carya, Tsuga, Fagus, Humulus, Celtis?,* Possible monolete fern spore	
	xx7: 16RLB009	tan claystone	Hog Cove Butte	44.1180, -116.6150		Poor-moderate	Taxodium/Cuppressaceae, *Pterocarya, Pinus, Juglans*	
	xx8: 16RLB010	organic-rich tan claystone	Hog Cove Butte	44.1190, -116.6160		Good	Chenopodiaceae, *Pterocarya, Ulmus/Zelkova, Carya?, Picea,* Taxodium/Cuppressaceae, *Betula?, Liquidambar, Pseudotsuga/Larix, Artemisia, Tilia?*	Equisetum
	xx9: 16RLB012 A	d. brown to black silt-claystone	Hog Cove Butte	44.1190, -116.6190		Good	Taxodium/Cuppressaceae, *Carya, Ulmus/Zelkova, Pterocarya, Humulus?, Juglans, Pinus, Picea, Alnus, Acer? Castenea*	
	xx9: 16RLB012 B	tan organic rich silt-claystone	Hog Cove Butte	44.1190, -116.6190		Good	Caryophyllaceae, Taxodium/Cuppressaceae, *Pinus, Alnus, Juglans, Pterocarya, Picea, Betula, Carya, Abies, Myriophyllum?, Ulmus/Zelkova, Pseudotsuga/Larix*	
	xx10: 15RLB027	claystone fossil frags	Paddock Valley, Equisetum site, FL7	44.1250, -116.6110		Moderate	*Taxus*, Taxodiaceae/ Cuppressaceae/Taxodium, *Pseudotsuga/Larix,* Chenopodiaceae, *Ulmus, Abies, Platanus, Pterocarya*	Equisetum, Unidentified seeds, *Platanus, Sassafras, Glyptostrobus*
	xx11: 15RLB030	fine sandstone	Paddock Valley, Metasequoia /Cercid site, FL1	44.2230, -116.5890		Poor-moderate	*Quercus*, Chenopodaceae, *Platanus, Pinus, Picea,* Taxodiaceae/Cuppressaceae/Taxodium	*Metasequoia, Cercidophyllum, Glyptostrobus, Fagas/Betula?*

	xx12: 15RLB031	tuffaceous siltstone	Paddock Valley, Great fossil leaf locality, FL4	44.1680, -116.6120		Good-excellent	*Picea*, Taxodiaceae/Cuppressaceae/Taxodium, *Abies, Alnus, Celtis? Quercus, Carya, Pterocarya, Liquidamber, Platanus, Cornus?, Acer, Ostrya, Betula, Tsuga, Onagraceae, Fagus, Tilia?, Juglans, Taxus*, Monolete spore, Trilete spore, *Nyssa?, Myrica?, Fraxinus*	*Cercidophyllum, Glyptostrobus, Metasequoia, Chamaecyparis, Lauraceae, Platanus, Taxodium, Sassafras, Lithocarpus, Quercus, Sequoia,* Equisetum, *Castenia?, Betula?*

Table 4

Formation Designation	Well	Measured Depth (MD)	Abies	Acer	Alnus	Artemesia	Asteraceae	Betula	Carpinus	Carya	Caryophyllaceae	Castenea	Cathaya	Cedrus	Chenopodeaceae	Compositae	Elaeagnus	Ephedra	Eriaceae	Fagus	Fraxinus	Fungal Spore	Ilex	Isoetes	Juglans	Juniperus	Liquidambar	Monolete spore	Moss	Nymphea	Nyssa	Onagraceae	Ostrya	Picea	Pinus	Poaceae	Podocarpus	Platanus	Pseudotsuga/Larix	Pterocarya	Rosaceae	Quercus	Salix	Sarcobatus	cf Saxifragaceae	cfTamarix	Taxus	TCT	Tilia	Trilete spore	Tsuga	Ulmus/Zelkova	cfVeronica
GF	IsCap	320					1							1	1					1					1									1	1					1		1									1		
	IsCap	1670	1	1	1	1				1	1									1	1				1					1	1			1	1	1		1	1	1		1	1				1	1				1	
	IsCap	1950	1	1	1		1			1							1							1	1			1			1		1	1	1		?	1		1		1								1		1	
CH	IsCap	2590			1					1	1	1			1														1				1	1	1				1	1								1			1	1	
	IsCap	3520	1		1					1					1		1					1			1		1	1						1	1					1							1	1	1			1	
PF	IsCap	4050	1	1	1															1					1		1						1	1				1		1		1						1				1	
Quat	Schwarz	130	1				1			1	1				1		1					1			1	1								1	1	1			1			1											
CH	Schwarz	870	1		1	1	1	1		1	1	1		1				1			1	1			1			1	1			1				1		1	1	1	1			1			1	1		1	1	1	1
	Schwarz	1330	1	1	1			1		1		1							1	1		1			1			1					1	1	1				1	1		1	1			1				1	1		
	Schwarz	1540	1	1	1					1					1					1													1		1					1									1			1	
PF	Schwarz	2060		1	1	1	1	1	1	1	1	1		1			1	1		1	1				1		1	1		1			1	1	1			1	1	1		1	1				1		1		1	1	
GF	State	630		1	1	1	1				1				1		1	1							1					1	1			1	1		1	1			1	1	1	1				1					
CH	State	1350				1	1	1						1	1																			1	1			1	1									1		1			
	State	3600	1	1							1		1		1	1											1										1	1				1			1			1					
PF	State	4230	1	1																			1		1		1							1				1		1				1									
	Espino	830			1		1	1							1		1	1		1					1					1				1	1	1						1						1				1	
GF	Espino	1160	1				1		1						1										1					1				1	1	1						1										1	
CH	Espino	1640	1	1	1		1		1	1							1								1									1	1	1		1		1		1										1	
	Espino	3170			1					1															1		1							1				1		1				1			1	1				1	
PF	Espino	3850	1				1	1								1	1								1			1						1	1			1	1	1			1	1				1				1	
	ML Invest	330	1			1	1	1	1						1		1			1					1						1			1	1	1						1	1					1	1				
GF	ML Invest	1330			1	1	1								1					1					1					1				1	1							1	1	1				1			1		
	ML Invest	1940	1							1		1																						1	1					1		1	1					1					
CH	ML Invest	2810	1			1	1						1												1			1						1	1			1					1	1								1	
	ML Invest	3880	1								1													1	1		1			1				1	1			1		1								1					
PF	ML Invest	4900	1																		1													1	1													1				1	

Figure 1

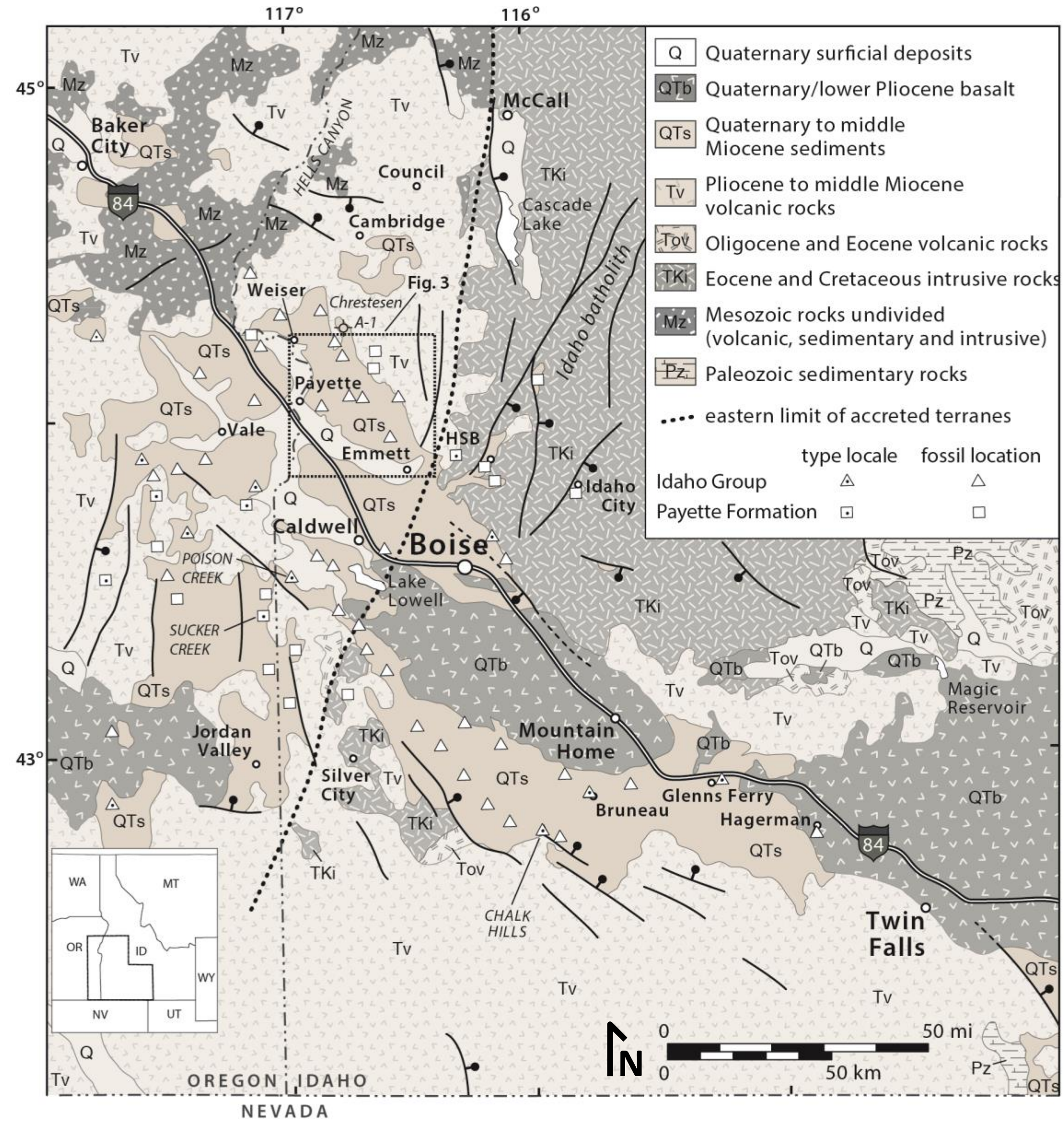

117°
116°
45°
43°
Q Quaternary surficial deposits
QTb Quaternary/lower Pliocene basalt
QTs Quaternary to middle Miocene sediments
Tv Pliocene to middle Miocene volcanic rocks
Tov Oligocene and Eocene volcanic rocks
TKi Eocene and Cretaceous intrusive rocks
Mz Mesozoic rocks undivided (volcanic, sedimentary and intrusive)
Pz Paleozoic sedimentary rocks
eastern limit of accreted terranes
type locale
fossil location
Idaho Group
Payette Formation
Baker City
McCall
Council
Cambridge
HELLS CANYON
Cascade Lake
Idaho batholith
Weiser
Chrestesen A-1
Fig. 3
Payette
Vale
Emmett
HSB
Idaho City
Caldwell
Boise
POISON CREEK
SUCKER CREEK
Lake Lowell
Magic Reservoir
Jordan Valley
Mountain Home
Silver City
Glenns Ferry
Bruneau
Hagerman
CHALK HILLS
Twin Falls
84
WA
MT
OR
ID
WY
NV
UT
N
0
50 mi
50 km
OREGON
IDAHO
NEVADA

Figure 2

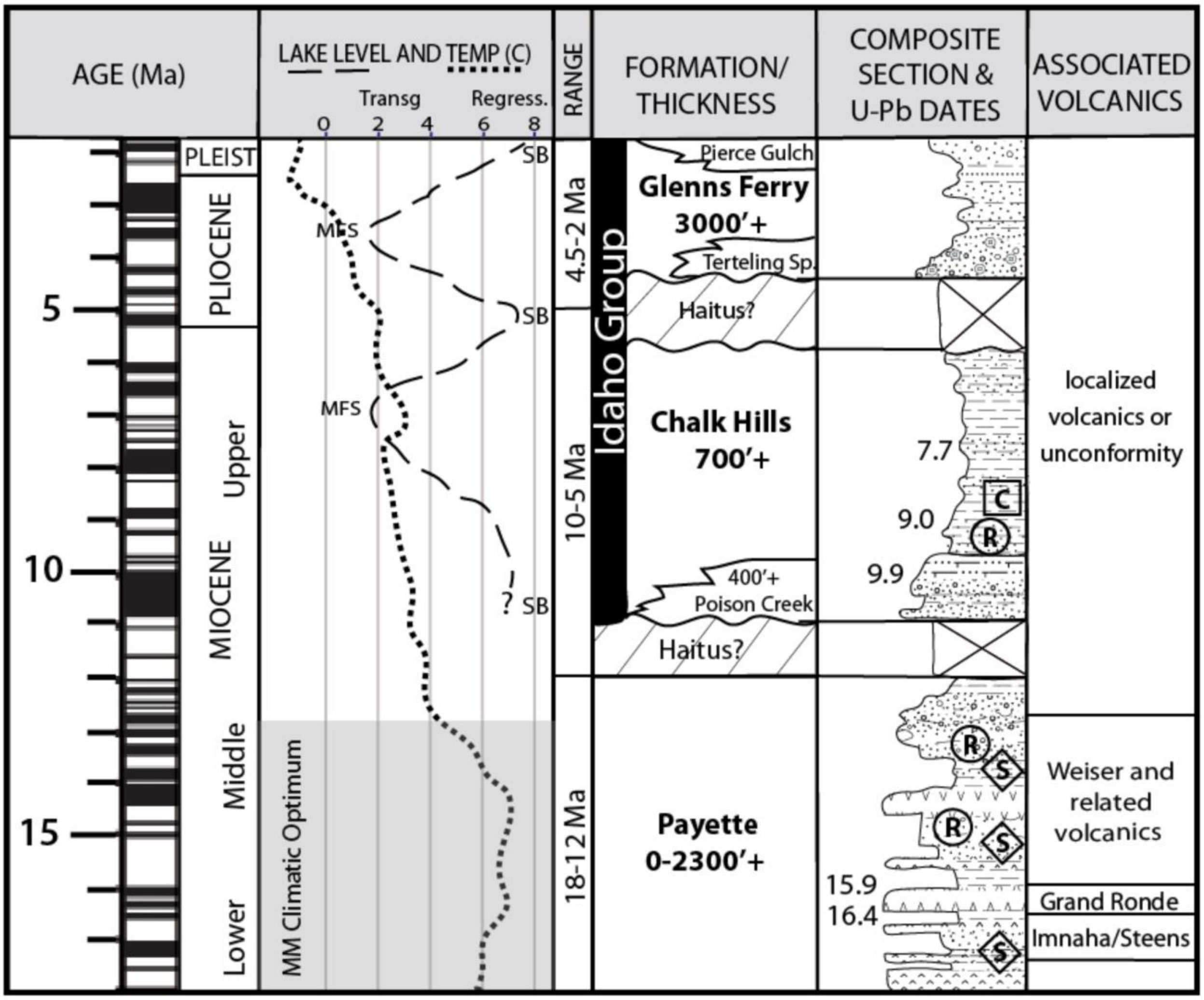

AGE (Ma)
LAKE LEVEL AND TEMP (C)
Transg
Regress.
0
2
4
6
8
RANGE
FORMATION/ THICKNESS
COMPOSITE SECTION & U-Pb DATES
ASSOCIATED VOLCANICS
PLEIST
PLIOCENE
MIOCENE
Upper
Middle
Lower
5
10
15
SB
MFS
SB
MFS
? SB
MM Climatic Optimum
4.5-2 Ma
10-5 Ma
18-12 Ma
Idaho Group
Pierce Gulch
Glenns Ferry 3000'+
Terteling Sp.
Haitus?
Chalk Hills 700'+
400'+ Poison Creek
Haitus?
Payette 0-2300'+
7.7
9.0
9.9
15.9
16.4
C
R
S
localized volcanics or unconformity
Weiser and related volcanics
Grand Ronde
Imnaha/Steens

Figure 3

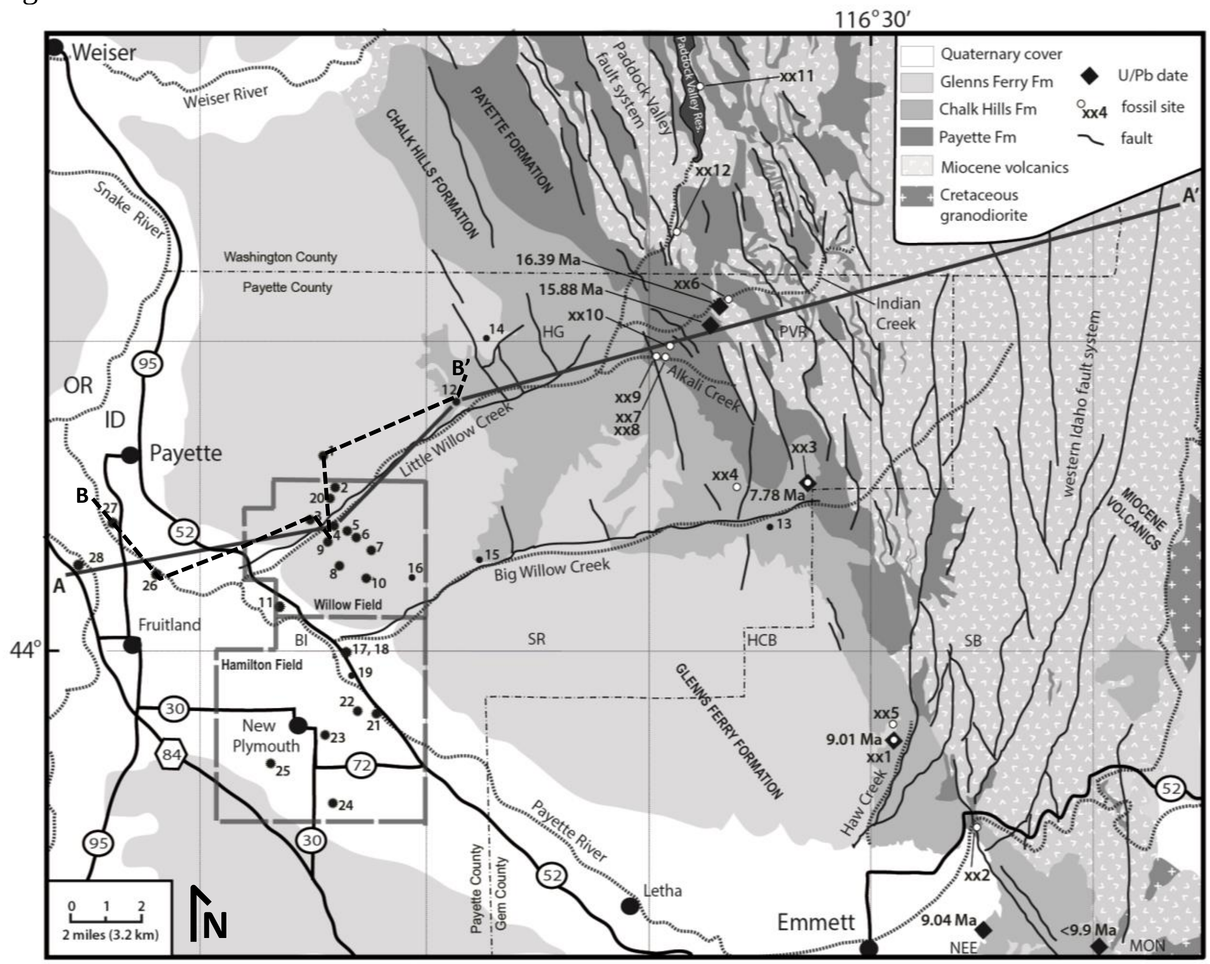

Hydrocarbon Wells

- ● Producing
- • Plugged and Abandoned

1 AM Idaho Kauffman1-34 2014, TD 5,800′

2 AM Idaho ML Investments 1-3 2015, TD 5,585′

3 AM Idaho Kauffman1-9 2014, TD 5,766′

4 Bridge Resources ML Investors 1-10 2010, TD 6,800′

5 AM Idaho ML Investments 2-10 2013, TD 4,996′

6 AM Idaho ML Investments 1-11 2014, TD 5,500′

7 Bridge Resources DJS Properties 2-14 2014, 5,500′

8 Bridge Resources DJS Properties 1-15 2010, TD 6,288′

9 AM Idaho ML Investments 3-10 2018, TD 5,000′

10 Bridge Resources DJS Properties 1-14 2010, 6,272′

11 AM Idaho Smoke Ranch 1-21 2013, TD 5,088′

12 Bridge Energy Island Capital 1-19 TD 4,385′

13 Bridge Resources Schwarz #1-10 2010, TD 2,602′

14 El Paso Nat. Gas-Oroco Oil Asmussen 1 1956, TD 4,015′

15 Standard American Co #2 Reins Estate 1975, TD 4,855′

16 Boise Petrol. Co No. 1 LW Kiene No. 1 1933, TD 2,500′

17 Oroco O&G Virgil Johnson #1 1955, TD 4,040′

18 Oroco O&G Virgil Johnson #2 1955, TD 3,522′

19 Oroco O&G Ted Daws #1 1955, TD 1,679′

20 AM Idaho ML Investments 2-3 2015, TD 5,034′

21 Bridge Resources Espino 1-2 2010, TD 4,500′

22 Bridge Resources Tracy Trust 3-2 2010, 2,815′

23 Bridge Resources White 1-10 2010, TD 2,415′

24 Bridge Resources Korn 1-22 2010, TD 2,324′

25 Bridge Resources State 1-17 2010, TD 4,519′

26 AM Idaho Barlow 1-14 2018, TD 4,150′

27 AM Idaho Fallon 1-10 2018, TD 4,519′

28 Ore-Ida Food Corp Ore-Ida No. 1 1979, TD 10,040′ (geothermal)

Figure 4

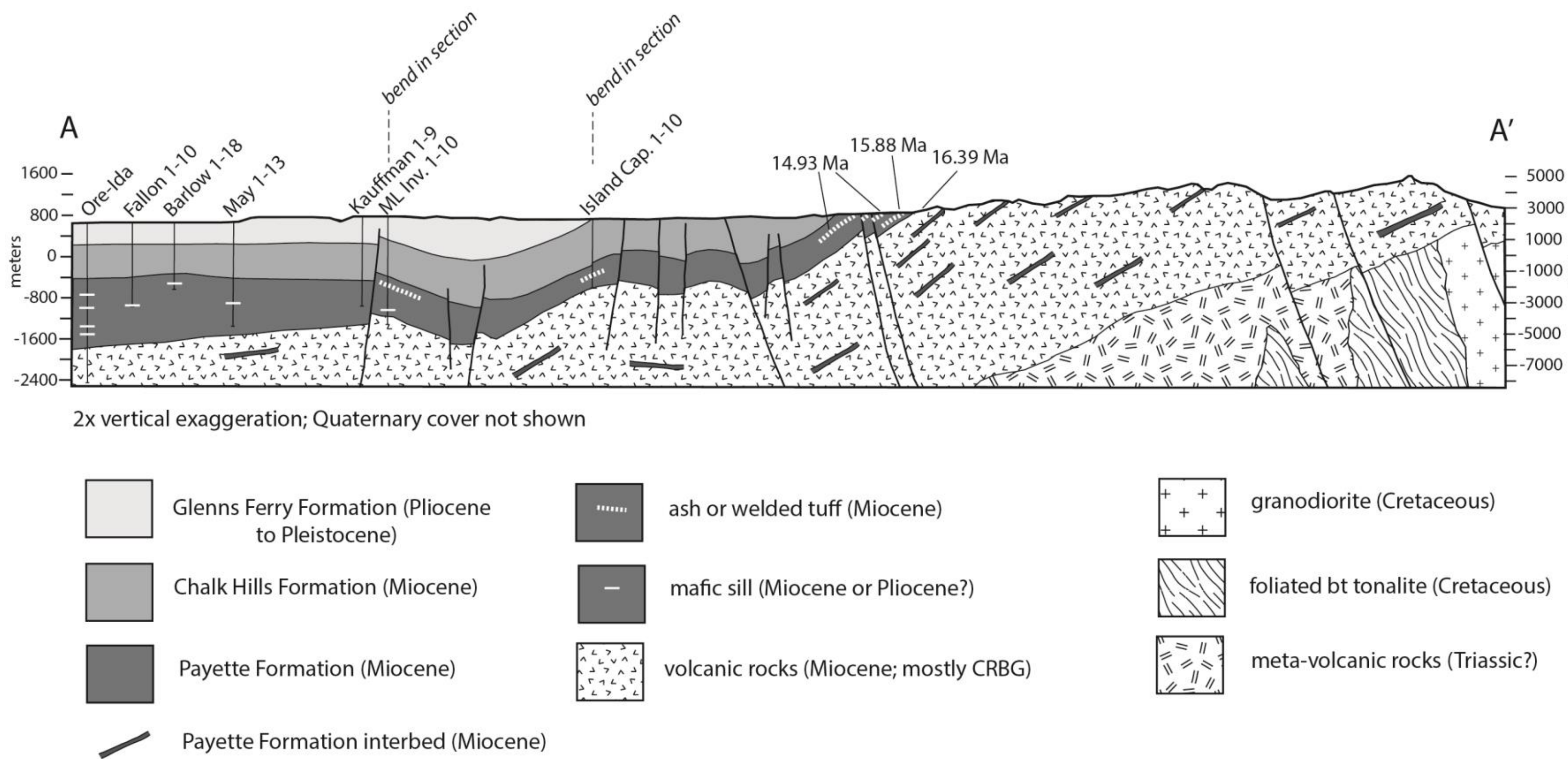

A
A′
bend in section
bend in section
Ore-Ida
Fallon 1-10
Barlow 1-18
May 1-13
Kauffman 1-9
ML Inv. 1-10
Island Cap. 1-10
14.93 Ma
15.88 Ma
16.39 Ma
meters
1600
800
0
-800
-1600
-2400
feet
5000
3000
1000
-1000
-3000
-5000
-7000
2x vertical exaggeration; Quaternary cover not shown
Glenns Ferry Formation (Pliocene to Pleistocene)
Chalk Hills Formation (Miocene)
Payette Formation (Miocene)
Payette Formation interbed (Miocene)
ash or welded tuff (Miocene)
mafic sill (Miocene or Pliocene?)
volcanic rocks (Miocene; mostly CRBG)
granodiorite (Cretaceous)
foliated bt tonalite (Cretaceous)
meta-volcanic rocks (Triassic?)

Figure 5

Formation Designation	Well	Measured Depth (MD)	Artemesia (A)	Asteraceae (B)	Caryophyllaceae	Cedrus (C)	Chenopodeaceae (D)	Ephedra €	Juniperus	Liquidambar (F)	Poaceae (G)	Platanus (H)	Pterocarya (I)
GF	IsCap	320		1		1	1						1
	IsCap	1670	1		1						1	1	1
	IsCap	1950		1								1	1
CH	IsCap	2590			1		1						1
	IsCap	3520					1			1			1
PF	IsCap	4050								1		1	1
Quat	Schwarz	130		1	1		1		1		1		
CH	Schwarz	870	1	1	1	1		1			1	1	1
	Schwarz	1330											1
	Schwarz	1540					1						1
PF	Schwarz	2060	1	1	1	1		1		1		1	1
GF	State	630	1	1	1		1	1				1	
CH	State	1350	1	1		1	1					1	
	State	3600			1		1			1		1	
PF	State	4230								1		1	1
	Espino	830		1			1	1			1		
GF	Espino	1160		1			1				1		
CH	Espino	1640		1							1	1	1
	Espino	3170								1		1	1
PF	Espino	3850		1								1	1
	ML Invest	330	1	1			1				1		
GF	ML Invest	1330	1	1			1						
	ML Invest	1940											1
CH	ML Invest	2810	1	1								1	
	ML Invest	3880			1					1		1	1
PF	ML Invest	4900											

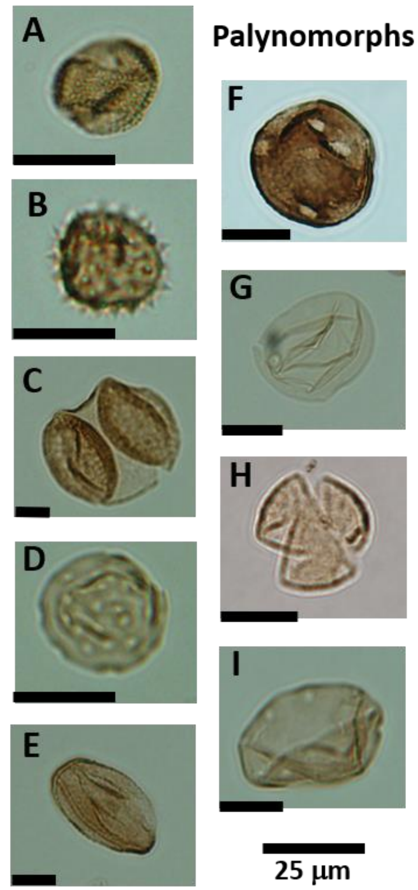

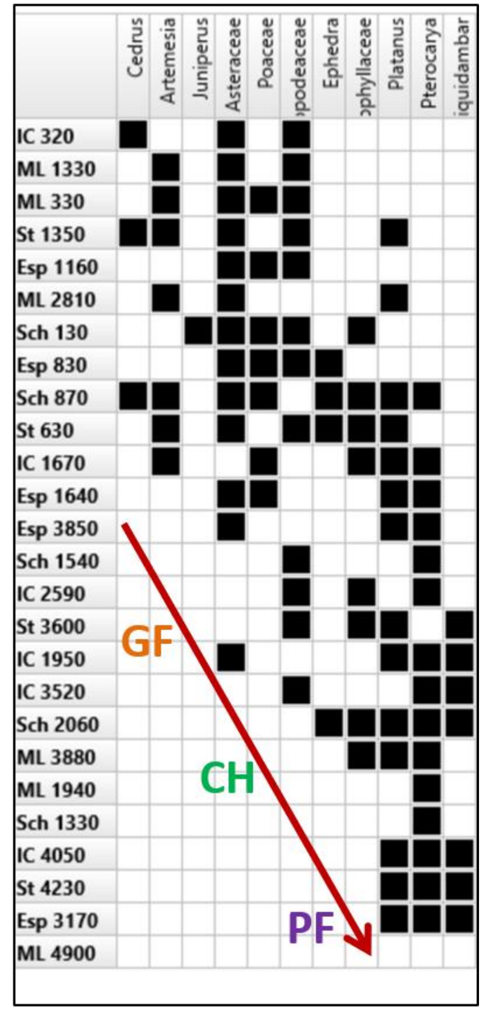

Figure 6

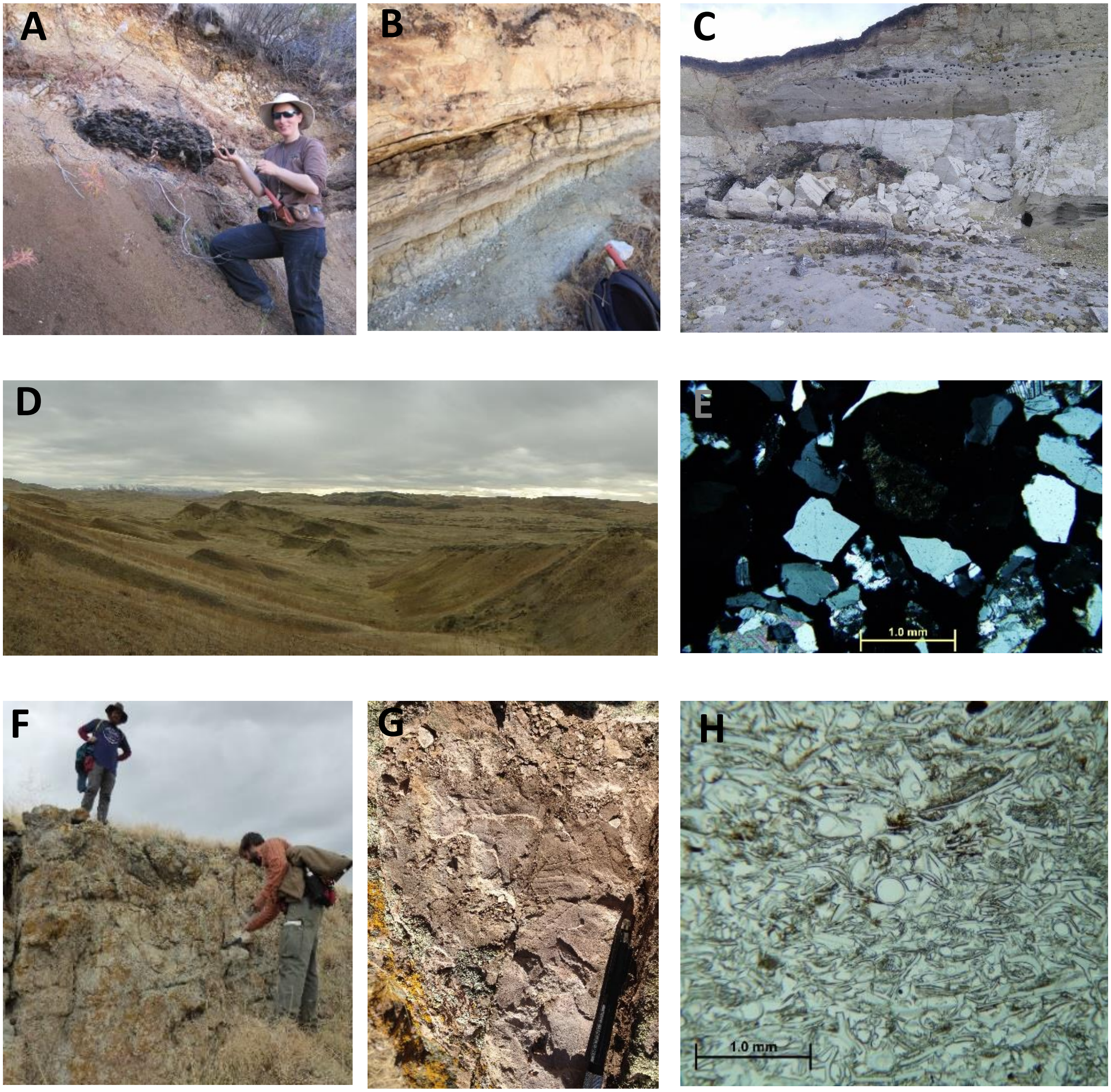

Figure 7

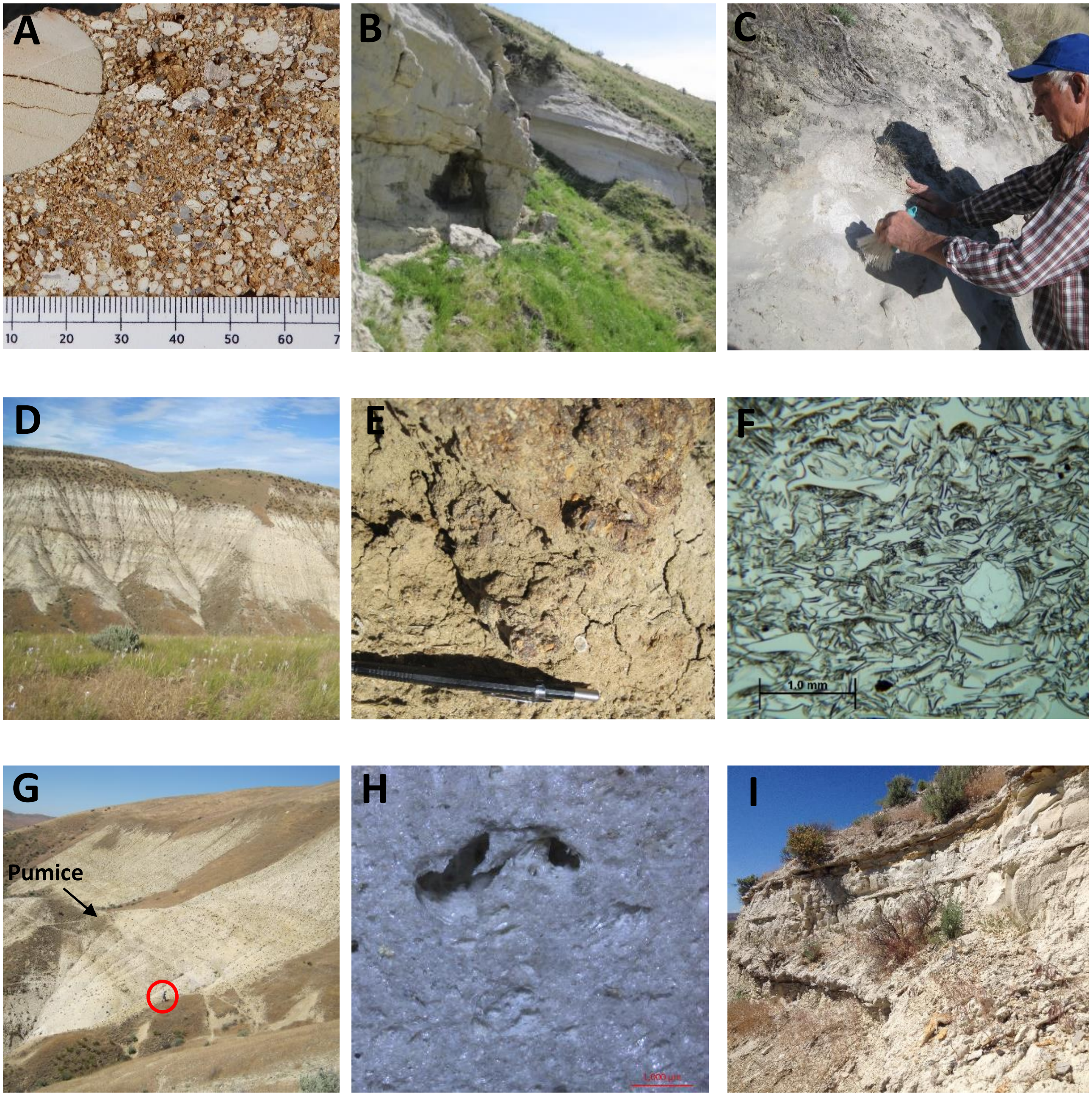

Figure 8

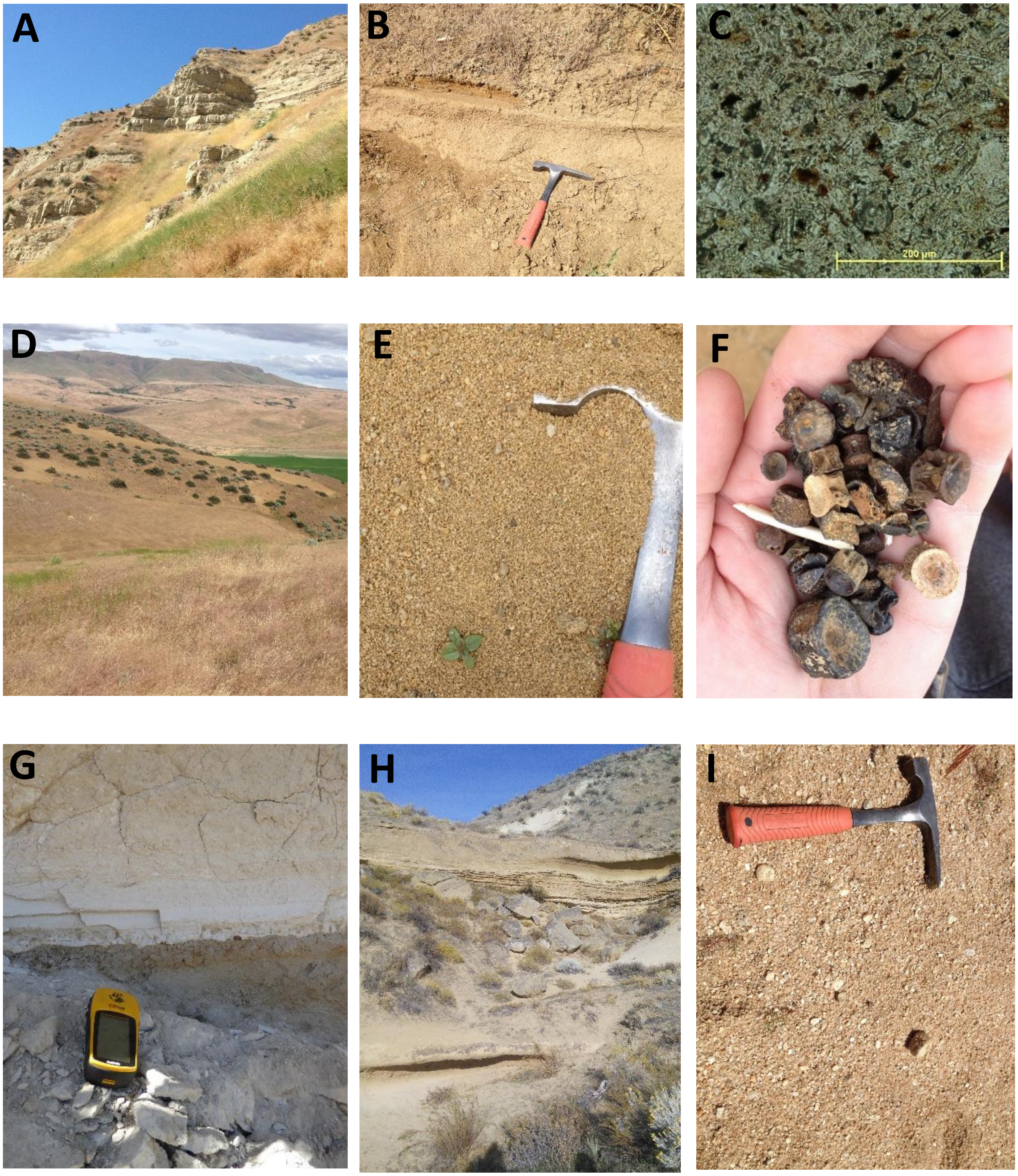

Figure 9

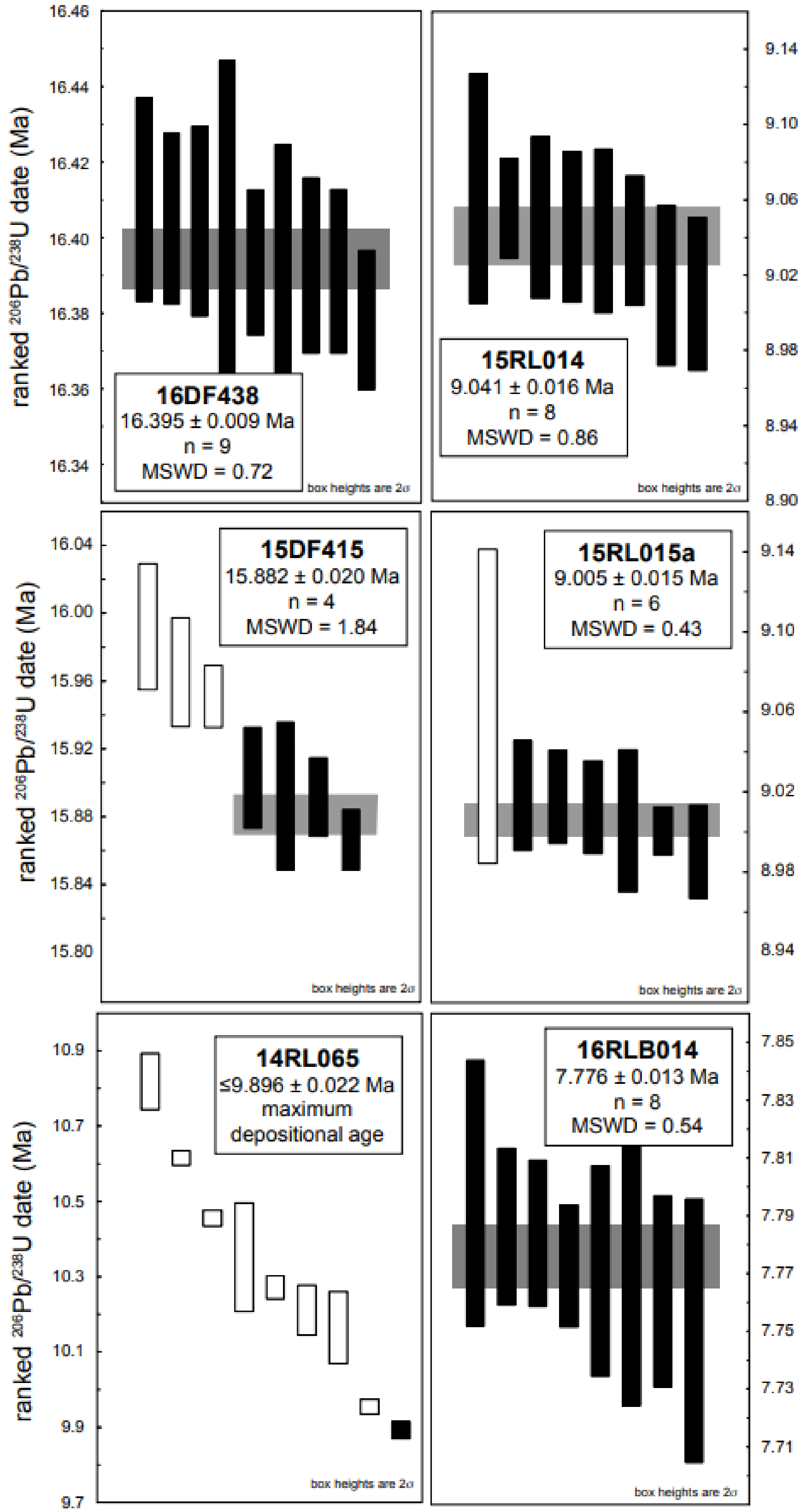
16DF438
16.395 ± 0.009 Ma
n = 9
MSWD = 0.72
15RL014
9.041 ± 0.016 Ma
n = 8
MSWD = 0.86
15DF415
15.882 ± 0.020 Ma
n = 4
MSWD = 1.84
15RL015a
9.005 ± 0.015 Ma
n = 6
MSWD = 0.43
14RL065
≤9.896 ± 0.022 Ma
maximum
depositional age
16RLB014
7.776 ± 0.013 Ma
n = 8
MSWD = 0.54
ranked ²⁰⁶Pb/²³⁸U date (Ma)
box heights are 2σ
16.46
16.44
16.42
16.40
16.38
16.36
16.34
9.14
9.10
9.06
9.02
8.98
8.94
8.90
16.04
16.00
15.96
15.92
15.88
15.84
15.80
9.14
9.10
9.06
9.02
8.98
8.94
10.9
10.7
10.5
10.3
10.1
9.9
9.7
7.85
7.83
7.81
7.79
7.77
7.75
7.73
7.71

Figure 10

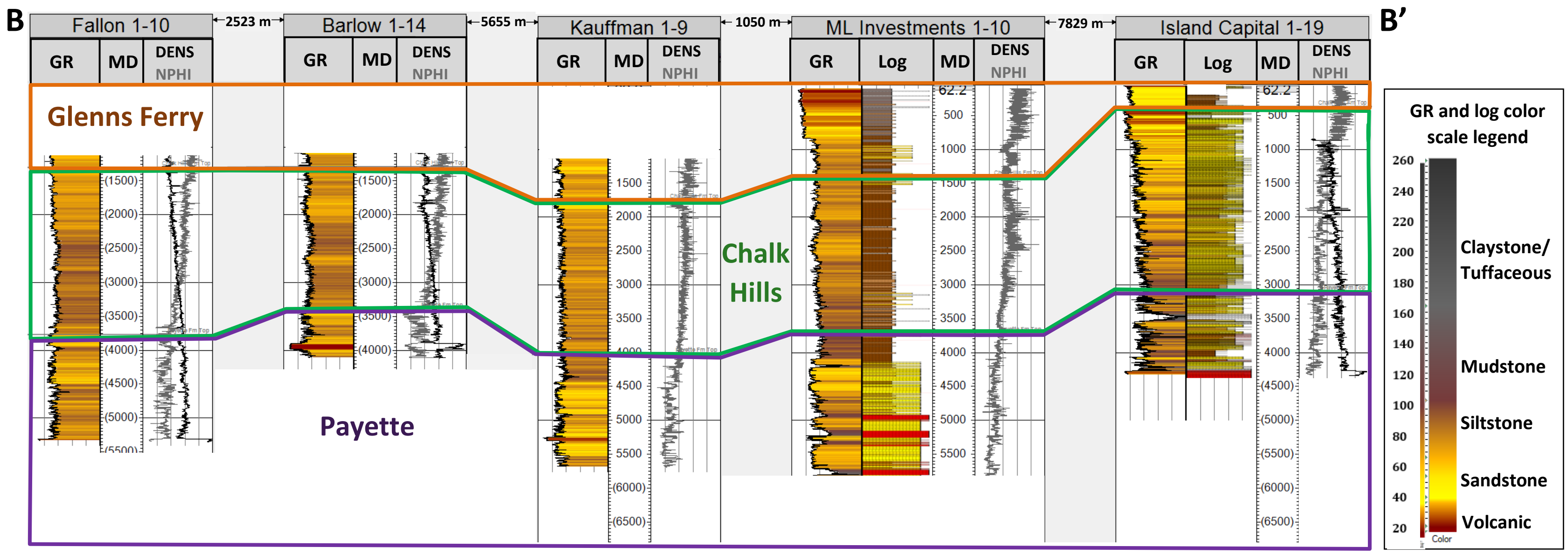
B
B'
Fallon 1-10
2523 m
Barlow 1-14
5655 m
Kauffman 1-9
1050 m
ML Investments 1-10
7829 m
Island Capital 1-19
GR
MD
Log
DENS
NPHI
Glenns Ferry
Chalk Hills
Payette
GR and log color scale legend
Claystone/ Tuffaceous
Mudstone
Siltstone
Sandstone
Volcanic

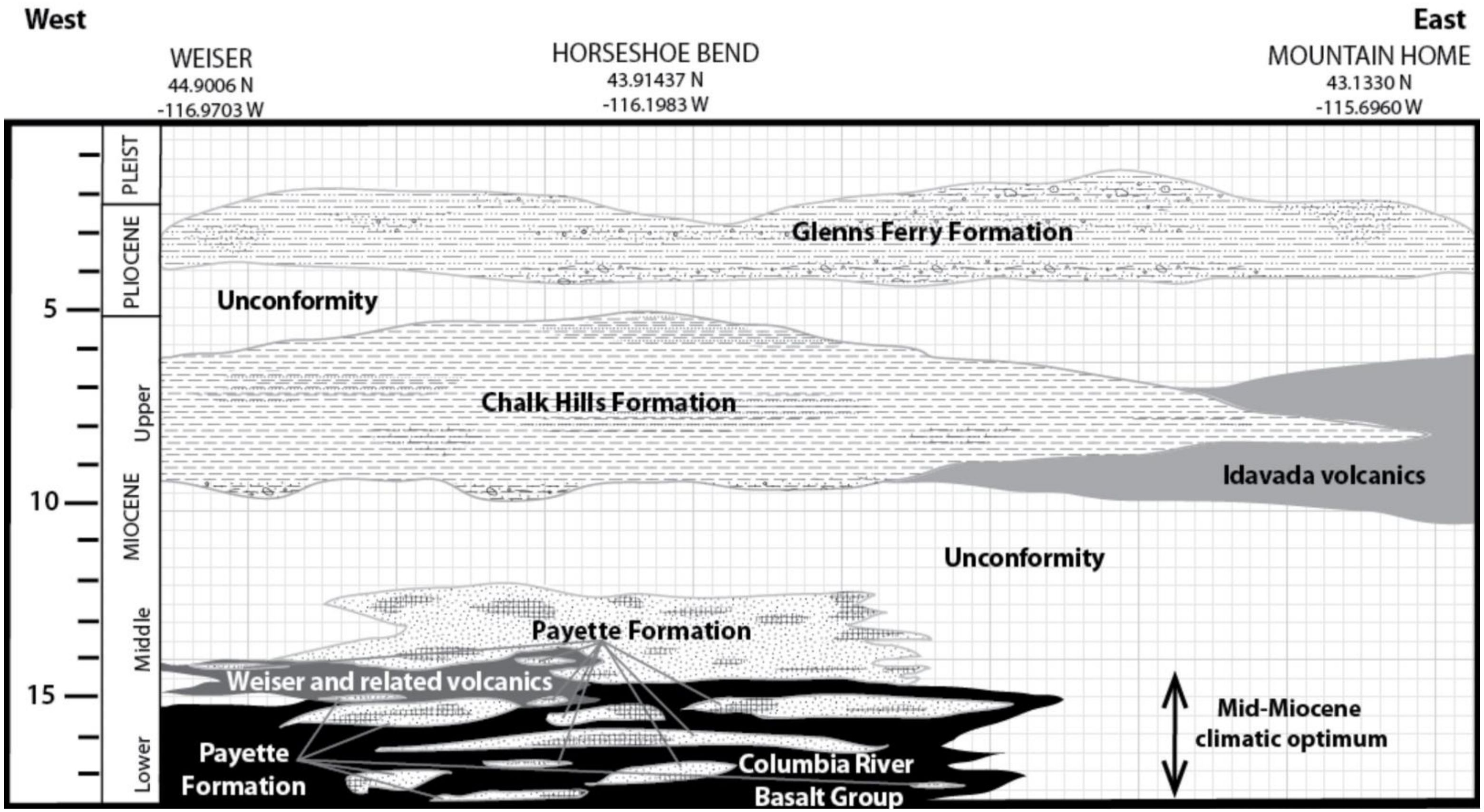

West
East
WEISER
44.9006 N
-116.9703 W
HORSESHOE BEND
43.91437 N
-116.1983 W
MOUNTAIN HOME
43.1330 N
-115.6960 W
PLEIST
PLIOCENE
MIOCENE
Upper
Middle
Lower
5
10
15
Glenns Ferry Formation
Unconformity
Chalk Hills Formation
Idavada volcanics
Unconformity
Payette Formation
Weiser and related volcanics
Mid-Miocene
climatic optimum
Payette
Formation
Columbia River
Basalt Group

Figure 11